Science of the Total Environment 848 (2022) 157345

Contents lists available at ScienceDirect

Science of the Total Environment

journal homepage: www.elsevier.com/locate/scitotenv

Deciphering natural and anthropogenic nitrate and recharge sources in arid region groundwater

Benjamin Linhoff

U.S. Geological Survey, New Mexico Water Science Center, Albuquerque, NM, United States of America

HIGHLIGHTS

- Major ions, isotopes, and CECs are used to decipher natural and anthropogenic NO_3^-.
- Subsoil NO_3^- reservoirs in arroyo floodplains are major source of groundwater NO_3^-.
- Artificial recharge in arid regions can be deciphered using ^3H, ^{14}C, and CECs.

GRAPHICAL ABSTRACT

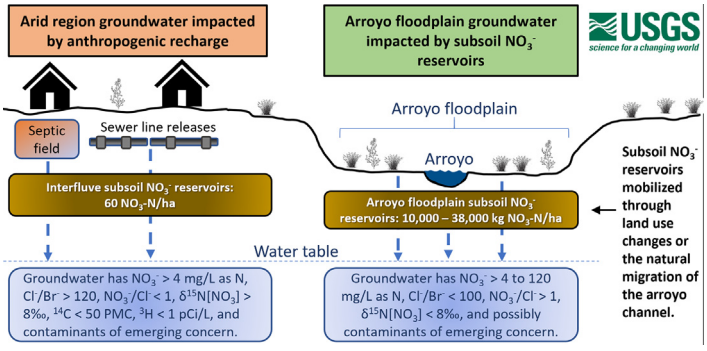

ARTICLE INFO

Editor: Jurgen Mahlknecht

Keywords:
Artificial sweeteners
CEC
Cl^-/Br^-
Artificial recharge
Nitrogen isotopes
Vadose zone nitrate

ABSTRACT

Recently, the subsoils of ephemeral stream (arroyos) floodplains in the northern Chihuahuan Desert were discovered to contain large naturally occurring NO_3^- reservoirs (floodplain: ~38,000 kg NO_3-N/ha; background: ~60 kg NO_3-N/ha). These reservoirs may be mobilized through land use change or natural stream channel migration which makes differentiating between anthropogenic and natural groundwater NO_3^- sources challenging. In this study, the fate and sources of NO_3^- were investigated in an area with multiple NO_3^- sources such as accidental sewer line releases and sewage lagoons as well as natural reservoirs of subsoil NO_3^-. To differentiate sources, this study used a large suite of geochemical tools including $\delta^{15}N[NO_3]$, $\delta^{18}O[NO_3]$, $\delta^{15}N[N_2]$, $\delta^{13}C[DIC]$, ^{14}C, tritium (^3H), dissolved gas concentrations, major ion chemistry, and contaminants of emerging concern (CEC) including artificial sweeteners. NO_3^- at sites with the highest concentrations (25 to 229 mg/L NO_3-N) were determined to be largely sourced from naturally occurring subsoil NO_3^- based on $\delta^{15}N[NO_3]$ (<8 ‰) and mass ratios of Cl^-/Br^- (<100) and NO_3^-/Cl^- (>1.5). Anthropogenic NO_3^- was deciphered using mass ratios of Cl^-/Br^- (>120) and NO_3^-/Cl^- (<1), $\delta^{15}N[NO_3]$ (>8 ‰), and CEC detections. Nitrogen isotope analyses indicated that denitrification is fairly limited in the field area. CEC were detected at 67 % of sites including ^3H dead sites (<1 pCi/L) with low percent modern carbon-14 (PMC; <30 %). Local supply wells are ^3H dead with low PMC; as ^3H does not re-equilibrate and ^{14}C is very slow to re-equilibrate during recirculation through infrastructure, sites with low PMC, ^3H < 1 pCi/L, and CEC detections were interpreted as locations with substantial anthropogenic groundwater recharge. Neotame was used to identify locations of very recent (<15 years before present) or ongoing wastewater influxes to the aquifer. This work shows the important influence of naturally occurring subsoil NO_3^- reservoirs on groundwater in arid regions and the major contribution of artificial recharge.

1. Introduction

Nitrate (NO_3^-) is the most common groundwater contaminant globally (Spalding and Exner, 1993). Elevated NO_3^- in drinking water can lead to

E-mail address: blinhoff@usgs.gov.

http://dx.doi.org/10.1016/j.scitotenv.2022.157345
Received 24 January 2022; Received in revised form 8 July 2022; Accepted 10 July 2022
Available online 23 July 2022

increased risk of methemoglobinemia (blue baby syndrome), colorectal cancer, and low birthweight outcomes (Schullehner et al., 2018; Sherris et al., 2021; Ward et al., 2018), while surplus nitrate loading to surface waters can contribute to eutrophication (Schindler, 2006). Excess NO_3^- in surface water and groundwater is largely due to the overuse of fertilizers and contamination by human and animal waste (Canter, 1996; Nolan et al., 2002). Natural NO_3^- sources such as atmospheric deposition, nitrogen (N) fixation in arid region soil crusts, termite mounds, and rock N can contribute a substantial amount of N in some watersheds (Houlton et al., 2018; Walvoord, 2010). In arid regions, large, naturally occurring NO_3^- reservoirs can occur in the subsoil, potentially a major source of NO_3^- to groundwater (Graham et al., 2008; Gutiérrez et al., 2018; Izbicki et al., 2015; Linhoff and Lunzer, 2021; B. Scanlon et al., 2008; Walvoord, 2010). In the American southwest, these reservoirs are generally the result of thousands of years of dry and wet atmospheric N deposition onto soils that have leached to the subsoil below plant root depth. Vadose zone NO_3^- deposits are susceptible to mobilization to underlying aquifers during land use or climate change, which can lead to excess groundwater NO_3^- (Linhoff and Lunzer, 2021; B. R. Scanlon et al., 2008; Walvoord et al., 2003). For mitigation of NO_3^-, sources must be identified and the potential for denitrification—the microbially mediated process whereby NO_3^- is ultimately transformed to N_2—should be assessed. Although there are many potential indicators of NO_3^- sources, successful discrimination is most likely if multiple tracers can be applied simultaneously.

Isotopes of NO_3^- ($\delta^{15}N$ [NO_3] and $\delta^{18}O$ [NO_3]) can be used to identify manure and human waste, while examining dissolved gas concentrations (N_2 and Ar) and isotopes ($\delta^{15}N[N_2]$) can determine the extent of denitrification (Böhlke et al., 2002). Analyzing both $\delta^{15}N$ and $\delta^{18}O$ in NO_3^- can help separate NO_3^- sources (Böttcher et al., 1990). For example, the $\delta^{15}N$ [NO_3] of soil organic N (ON) is +3 ‰ to +8 ‰ while mineral fertilizers are between −8 ‰ and +7 ‰. While there is some overlap, measuring $\delta^{15}N[NO_3]$ can be especially helpful in identifying manure and human wastewater sources, which have values between +5 ‰ to +35 ‰ (Nikolenko et al., 2018). These differences result from microbially driven reactions such as assimilation, nitrification, and denitrification, which almost always result in ^{15}N enrichment of the substrate and depletion of the product (Nikolenko et al., 2018). $\delta^{18}O[NO_3]$ values in groundwater can also be indicative of NO_3^- sources and processes. For example, synthetic NO_3^- fertilizers, which are derived from atmospheric N_2, have $\delta^{18}O$ values close to atmospheric (+23.5 ‰; Hollocher, 1984). During denitrification, $\delta^{18}O[NO_3]$ increases as denitrifying bacteria prefer the lighter O isotope leaving the residual heavier. During nitrification, one O atom from dissolved O_2 and two atoms from water are combined to form NO_3^-, hence $\delta^{18}O[NO_3]$ is controlled by nitrification, denitrification, and the $\delta^{18}O$ value of the reactant water (Kendall and Aravena, 2000).

Carbon isotope systems can be useful in estimating groundwater age and inferring groundwater sources, identifying recent recharge and areas vulnerable to contamination, and helping to differentiate between background and anthropogenically impacted sites (Geyh, 2000; Grundl et al., 2013; Han and Plummer, 2016; Jasechko et al., 2017). Further analyzing C isotopes and associated major ion chemistry can also help determine whether bicarbonate (HCO_3^-) is sourced from carbonate mineral dissolution or the oxidation of organic matter during O_2 reduction or denitrification (Han et al., 2012; Han and Plummer, 2016). Tritium (^3H) is often used as an indicator of recently recharged groundwater (Lindsey et al., 2019). Concentrations of ^3H in groundwater are affected by groundwater depth, timing of recharge relative to bomb ^3H inputs (mainly between 1952 and 1963), and its half-life (12.32 years; Eastoe et al., 2012).

Domestic and municipal wastewater may carry distinct chemical signatures such as high Cl^-/Br^- ratios (Davis et al., 1998). In general, domestic wastewater and municipal sewage has Cl^-/Br^- ratios between 300 and 1100 (by mass) while the Cl^-/Br^- ratio in non-impacted groundwater is typically <100 (Davis et al., 1998; Katz et al., 2011). Because of the conservative nature of Cl^- and Br^- and the simplicity of using elemental ratios, Cl^-/Br^- ratios are often used as a first step to identify waters impacted by sewage effluent (Katz et al., 2011). The ratio of total nitrogen (TN) to Cl^- is typically ~11 (by mass) from bulk atmospheric deposition (National Atmospheric Deposition Program, 2022). Anthropogenic wastewater and fertilizers can contribute both Cl^- and NO_3^- with impacted groundwater generally having NO_3^-/Cl^- ratios <0.5 because by mass, more Cl^- is generally contributed than NO_3^- (Sapek, 2002; Stites and Kraft, 2001). It should be noted that as NO_3^- is subject to redox reactions, care must be taken when interpreting NO_3^-/Cl^- ratios as changes along a flow path may be due to denitrification (Lowrance, 1992).

Contaminants of emerging concern (CEC)—artificial sweeteners, pharmaceuticals, and wastewater indicators (WWI)—are useful as tracers of anthropogenic NO_3^- sources and serve as tracers of post-industrial revolution aquifer recharge (McCance et al., 2018). Artificial sweeteners are also increasingly being recognized as pollutants and may result in substantial ecotoxicity (Luo et al., 2019). Since saccharin was first discovered in 1879 (Fahlberg and Remsen, 1879), artificial sweeteners have become widely popular globally as sugar substitutes used in food, beverages, pharmaceuticals, personal care products, and even animal feed (Buerge et al., 2009; Gan et al., 2013; Van Stempvoort et al., 2011). Their usefulness in groundwater studies stems from their typically highly recalcitrant behavior making them suitable tracers of anthropogenic waste (Buerge et al., 2009; Robertson et al., 2016). This stability in the environment varies between sweeteners with acesulfame-K generally being the most persistent (Buerge et al., 2009) while sucralose, aspartame, and neotame degrade more readily (Margot et al., 2015). In the United States, neotame was approved for consumption in 2002, acesulfame-K in 1988, sucralose in 1998, and saccharin in 1879 (U.S. Food and Drug Administration, 2018). Hence, their presence in groundwater can help better constrain the timeline of contamination. Human-use pharmaceuticals are also widely distributed in groundwater and surface waters and can serve as additional tracers of anthropogenic water sources and recent groundwater recharge (Bexfield et al., 2019; Glassmeyer et al., 2008; Richardson and Ternes, 2011). Many of these compounds are present in both domestic wastewater and in effluent from wastewater treatment facilities because treatments are often not designed to remove these compounds (Vidal-Dorsch et al., 2012).

This work uses major ion ratios, dissolved gases, stable and radioactive isotopes, and a wide variety of CEC to differentiate NO_3^- sources in the impacted aquifers in and around KAFB. With a few exceptions (e.g. McCance et al., 2020, this breadth of techniques has rarely been used to separate NO_3^- sources. Due to the extent of analyses, this work provides an opportunity to compare techniques in understanding NO_3^- impacted aquifers.

2. Study area

Arroyos—dry creek beds in the American Southwest that flow after sufficient rainfall—were recently discovered to contain unusually large reservoirs of subsoil NO_3^- in their floodplains (Linhoff and Lunzer, 2021). Linhoff and Lunzer (2021) describe large NO_3^- subsoil reservoirs (10,000–38,000 kg NO_3-N/ha) in an arroyo floodplain on Kirtland Air Force Base (KAFB) near Albuquerque, New Mexico, USA (Figs. 1 and S1). Nitrate accumulation in the arroyo floodplain is attributed to the evaporation of water infiltrating the arroyo channel sediments, and the lateral movement and evaporation of water through subsoils from beneath the arroyo channel to the surrounding floodplain. Enhanced nitrification during wetting and drying in the arroyo channel (Gómez et al., 2012) and high NO_3^-/Cl^- ratios (~11 by mass) measured in atmospheric deposition may account for the very high NO_3^-/Cl^- ratios (5–30) measured in subsoil porewaters in the floodplain (Linhoff and Lunzer, 2021). Based on modeling, this process of naturally accumulating NO_3^- in the subsoils of the floodplain was estimated to occur in 200 to 800 years or eight to 75 times faster than through atmospheric deposition alone. Arroyo channel migration across the floodplain—a process that can be observed in historical satellite photos occurring on decadal timescales (Linhoff and Lunzer, 2021)—likely periodically flushes the arroyo floodplain subsoil NO_3^- to the underlying aquifers. Subsequent water flows through the arroyo channel and

evaporation in subsoils in the floodplain likely act to regenerate NO_3^- deposits over the course of hundreds of years. Hence, arroyo floodplains should be considered as potential NO_3^- sources to groundwater in arid regions.

Though NO_3^- contamination of groundwater is generally less likely in arid regions with thick unsaturated zones (Nolan et al., 2002), elevated groundwater NO_3^- is widespread in northern and central New Mexico (Linhoff et al., 2016; McQuillan, 2004). In particular, NO_3^- contamination in the aquifer beneath KAFB is a major concern (Copland, 2019). In addition to subsoil NO_3^- reservoirs in arroyo floodplains, numerous anthropogenic sources of nitrate have been identified on and around KAFB including landfills, sewer line releases, and former leach fields (Fig. 1; Oneida Total Integrated Enterprises, 2014). A historic neighborhood on the northeast border of KAFB was not connected to municipal sewer systems until relatively recently and hence, there may be former septic leach fields and tanks that could be an off-base NO_3^- source to KAFB. West of KAFB in the floodplain of Tijeras Arroyo (Fig. 1), extremely high groundwater NO_3^- concentrations (>100 mg/L NO_3-N) have been observed in Albuquerque's Mountain View community (Mohr, 2009; Thomson and McQuillan, 1984). These high NO_3^- concentrations resulted in one case of methemoglobinemia prior to the community being connected to municipal water supply (Mohr, 2009; Thomson and McQuillan, 1984). While the anthropogenic NO_3^- sources in and around KAFB are numerous, high NO_3^- in groundwaters beneath the arroyo floodplain on KAFB tend to have NO_3^-/Cl^- ratios far higher than background sites and low Cl^-/Br^- ratios suggesting a subsoil NO_3^- source (Linhoff and Lunzer, 2021).

The majority of groundwater samples collected for this study were from aquifers of the Santa Fe Group (Fig. S1), a thick (~2.7 km) basin-fill sediment sequence that formed in the late Oligocene to middle Pleistocene; it consists of piedmont-slope and fluvial basin-floor deposits derived from the surrounding uplifts (Haase and Lozinsky, 1995). The study area is bisected by multiple north-south trending faults that are part of the Tijeras Fault Complex. These faults are generally parallel to the mountain block on the eastern side of the Rio Grande Valley. Several springs—sampled for this study—are associated with these faults including Hell Canyon Tank and Hubble Spring (Fig. 1), both of which may contain groundwater from the Santa Fe Group aquifers or deeper groundwater (Haase and Lozinsky, 1995).

Two aquifers exist within the upper Santa Fe Group, a perched system and the regional aquifer (Copland, 2017). The perched aquifer system has an extent of ~9 km^2, largely within KAFB (Fig. 1); the perching layer consists of multiple lenses of alluvial-fan clay and silt. Vertical groundwater flow is minimal because of lenticular clay units; groundwater flow direction in the perched system is generally to the southeast. The perched system merges with the regional aquifer at its southeastern extent (Fig. S1). Flow through the floodplain is generally from the east to the west moving downhill from the mountain front to the Rio Grande. Prior to World War II, the perched aquifer likely only contained minimal water (Copland, 2017). When KAFB and Sandia National Laboratory (located within KAFB) began operations in 1941, various anthropogenic inputs including sewage impoundments, septic leach fields, outfall ditches, landscape watering, leaking water lines, and a golf course likely increased infiltration and created or enhanced the perched aquifer (Copland, 2017).

Prior to large scale regional aquifer withdrawals in the City of Albuquerque, groundwater flow directions in the regional aquifer were north to south, with a westward flow direction near the mountain-front boundaries to the east (Bexfield and Anderholm, 2002; Plummer et al., 2012). However, groundwater pumping by the City of Albuquerque and to a lesser extent KAFB, has altered groundwater flow directions and now groundwater generally flows to the west and northwest through KAFB (Galanter and Curry, 2019) with significant recharge around the KAFB golf course and east of the West Sandia Fault (Copland, 2017). Notably, while the regional groundwater flow is generally towards the west and northwest, groundwater in the perched system moves in the opposite direction towards the southeast (Copland, 2017).

3. Methods

3.1. Collection of groundwater and surface water samples

Fifty-five sites were sampled for this study including two streams, one ephemeral stream, three springs, and 49 groundwater sites (Tables 1 and S1). Sampling locations were chosen to be spatially representative of groundwater and surface water within the study area and cover regions with elevated and low nitrate concentrations. Across the study area, 35 samples were collected from the regional Santa Fe Group aquifer. In addition to 22 samples on KAFB collected in the regional aquifer, nine samples were collected in the perched aquifer and one sample, (TJA-4), was collected in the mixing zone above the regional aquifer and beneath the perched aquifer. KAFB-0615 on the eastern side of KAFB and EGC-01 and EGC-17 east of KAFB were collected in the fractured granite mountain-front aquifer. To provide comparison, background sites located on the eastern portion of Isleta Pueblo Reservation (ASL PD and UES-4) were sampled as there is no known source of anthropogenic nitrate to these sites. All sites sampled on Isleta Pueblo were on rangeland used for grazing cattle. All sites were sampled once except for the ephemeral stream Tijeras Arroyo which was sampled four times following rainfall events. Details of surface water and groundwater collection methods are described in S.1, and quality assurance and control samples are described in S.2.

3.2. Major element and nitrogen species analyses

All samples collected were analyzed for nitrogen species and major element composition (Tables 1 and S2). These samples were stored at 4 °C until analysis. Samples for nitrogen species—organic nitrogen (ON), $NH_3^\circ + NH_4^+$, NO_2^-, and NO_3^-—were filtered to 0.45 μm and collected in 125 mL brown polyethylene bottles before being analyzed within 30 days of collection. $NH_3^\circ + NH_4^+$, NO_2^-, NO_3^- were measured through colorimetric determinative methods while ON were measured using titrimetric digestion-distillation methods (Fishman, 1993; Patton and Kryskalla, 2011). Samples collected for major cations were filtered to 0.45 μm, acidified to pH < 2, and stored chilled until analysis using inductively coupled plasma mass spectrometry (Fishman, 1993). Major anion samples were filtered to 0.45 μm and chilled until analysis using ion-exchange chromatography (Fishman, 1993). Carbonate species (H_2CO_3, HCO_3^-, and CO_3^{2-}) were inferred from field alkalinity titrations. All nutrient and major element analyses were completed at the U.S. Geological Survey (USGS) National Water Quality Laboratory in Lakewood, CO.

3.3. Contaminants of emerging concern methods

Thirty-eight samples were measured for WWI chemicals including 69 compounds typically found in domestic and industrial wastewater, including the alkylphenol ethoxylate nonionic surfactants and their degradates, food additives, fragrances, antioxidants, flame retardants, plasticizers, industrial solvents, disinfectants, fecal sterols, polycyclic aromatic hydrocarbons, and high-use domestic pesticides (Table S3). Additionally, 36 samples were measured for 110 common human-use pharmaceutical compounds (Table S3). These include common drugs such as Metformin, Acetaminophen, Carbamazepine, and Albuterol.

Sample collection for pharmaceutical and WWI samples followed USGS guidelines outlined in Section 5.6.1F of the USGS National Field Manual (USGS, variously dated). Briefly, pharmaceutical samples were filtered to 0.7 μm and collected in 20-mL amber glass, stored at 1–5 °C in the dark, then analyzed within nine days of collection. Pharmaceuticals were measured through direct injection into a high-performance liquid chromatograph coupled to a triple-quadrupole tandem mass spectrometer using an electrospray ionization source operated in the positive ion mode (Furlong et al., 2014). WWI compounds were analyzed from whole unfiltered water samples collected in baked 1-L amber glass bottles. These samples were extracted within 14 days of collection and analyzed through liquid-

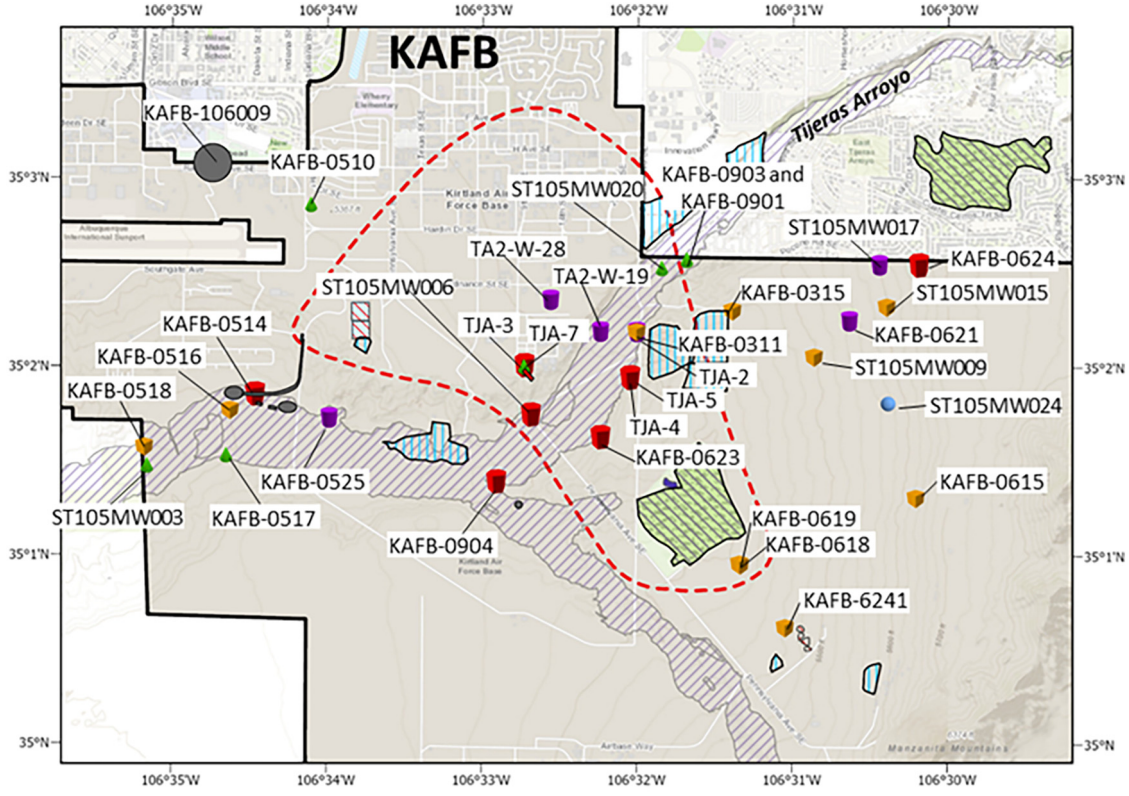
KAFB
Tijeras Arroyo
KAFB-106009
KAFB-0510
KAFB-0903 and
KAFB-0901
ST105MW020
ST105MW017
KAFB-0624
TA2-W-28
TA2-W-19
ST105MW006
KAFB-0315
ST105MW015
KAFB-0514
TJA-3
TJA-7
KAFB-0621
KAFB-0516
KAFB-0311
ST105MW009
KAFB-0518
TJA-2
TJA-5
ST105MW024
TJA-4
KAFB-0623
KAFB-0525
KAFB-0615
ST105MW003
KAFB-0517
KAFB-0619
KAFB-0904
KAFB-0618
KAFB-6241
106°35'W
106°34'W
106°33'W
106°32'W
106°31'W
106°30'W
35°3'N
35°2'N
35°1'N
35°N

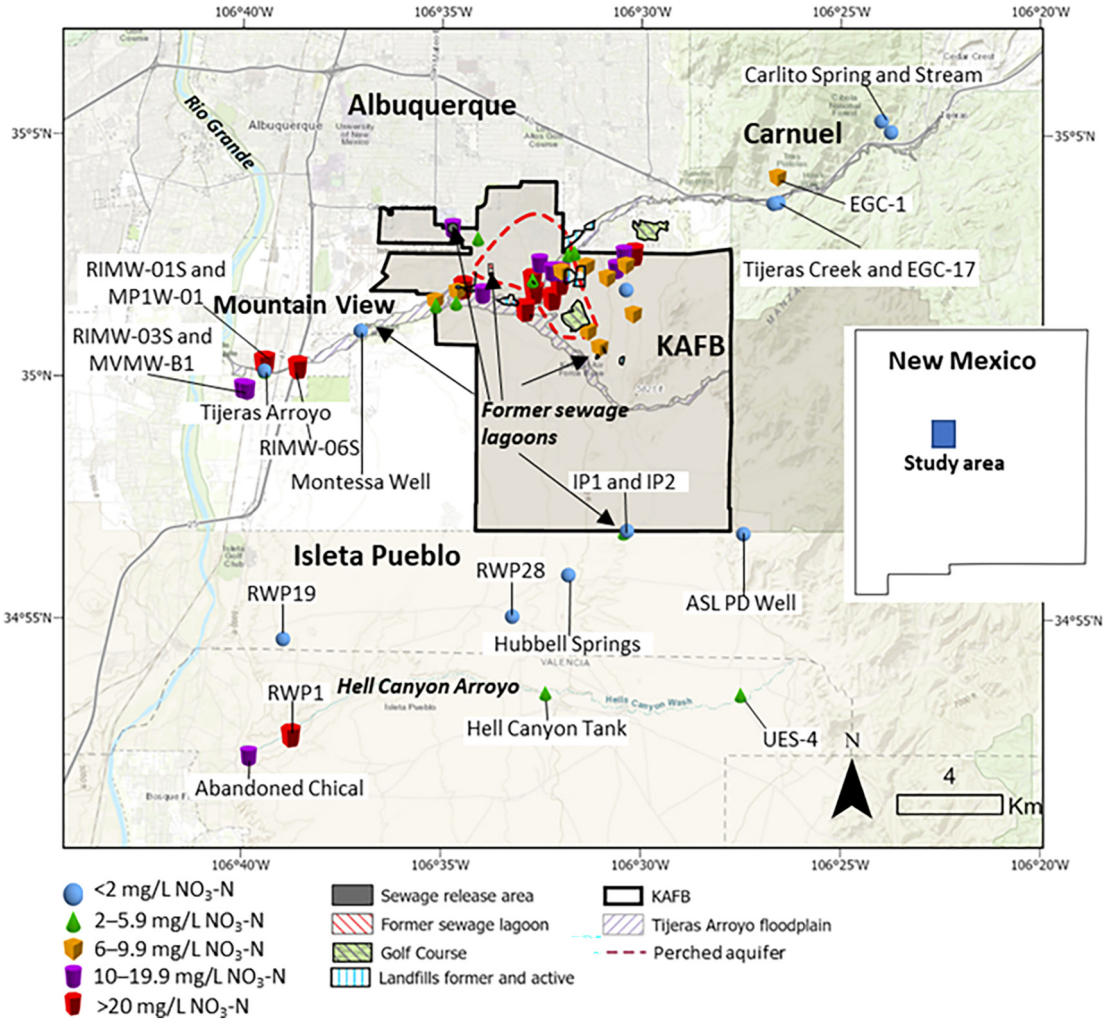
Albuquerque
Rio Grande
Carlito Spring and Stream
Carnuel
EGC-1
Tijeras Creek and EGC-17
RIMW-01S and
MP1W-01
Mountain View
RIMW-03S and
MVMW-B1
KAFB
Tijeras Arroyo
RIMW-06S
Montessa Well
Former sewage
lagoons
IP1 and IP2
New Mexico
Study area
Isleta Pueblo
RWP28
RWP19
ASL PD Well
Hubbell Springs
RWP1
Hell Canyon Arroyo
Hell Canyon Tank
UES-4
N
4
Km
Abandoned Chical
106°40'W
106°35'W
106°30'W
106°25'W
106°20'W
35°5'N
35°N
34°55'N
<2 mg/L NO3-N
2–5.9 mg/L NO3-N
6–9.9 mg/L NO3-N
10–19.9 mg/L NO3-N
>20 mg/L NO3-N
Sewage release area
Former sewage lagoon
Golf Course
Landfills former and active
KAFB
Tijeras Arroyo floodplain
Perched aquifer

liquid extraction and capillary-column gas chromatography/mass spectrometry (Zaugg et al., 2006).

All samples collected were analyzed for artificial sweeteners (Table S3); artificial sweetener analyses were completed on filtered (0.45 μm) water. Each sample was split into five 125-mL amber glass bottles, filled halfway, and frozen following sample collection. Artificial sweetener samples were analyzed at the USGS Organic Geochemistry Research Laboratory in Lawrence, KS. Analysis was performed using solid-phase extraction and ultra-performance liquid chromatography/tandem mass spectrometry (UPLC/MS/MS) with electrospray ionization using multiple reaction monitoring. Details of artificial sweetener analyses can be found in S.3. Details of data censoring and blank results for other CECs are presented in Table S4 and S.4 and S.5.

3.4. Dissolved gas concentration

Forty-eight groundwater samples were analyzed for dissolved N_2, argon (Ar), methane (CH_4), and O_2 gas using a Hewlett Packard model 7890B gas chromatograph (Table S5). These samples were collected in pre-weighed 150-mL septum bottles. For preservation of bioactive constituents, potassium hydroxide was added to the bottles to increase pH to >10. Sample discharge tubing, flowing at a rate of ~1 L/min, was placed at the bottom of the 150-mL sample bottles and allowed to cycle water for one minute; bottles were submerged in a 4-L bucket overflowing with raw water during collection. After ensuring no bubbles were trapped inside of the bottle, the bottle was sealed underwater with a needle through the septum. Samples were collected in duplicate, stored on ice, and shipped overnight in coolers to the USGS Reston Groundwater Dating Laboratory. Details of laboratory analyses of dissolved gases can be found in S.6.

3.5. Isotopic analyses of nitrate and nitrogen gas

Fifty-four samples analyzed for $\delta^{15}N[NO_3]$ and $\delta^{18}O[NO_3]$ were filtered to 0.2 μm and collected in 125-mL polyethylene bottles (Table 1). Samples were placed on ice and immediately shipped to the USGS Stable Isotope Laboratory to be analyzed. For analysis, dissolved NO_3^- was converted to nitrous oxide (N_2O) by denitrifying bacteria (*Pseudomonas aureofaciens*) and the N_2O was analyzed for N and O isotopic abundance by continuous-flow isotopic-ratio mass spectrometry (Sigman et al., 2001). The isotopic composition of dissolved N_2 was determined for 45 groundwater samples by gas chromatograph separation and continuous flow isotope ratio mass spectrometry on headspace gas leftover after gas chromatograph analysis of dissolved gas concentrations. N isotope ratios are reported in per mil (‰) relative to N_2 in air (Mariotti, 1983). Oxygen isotope ratios are reported in ‰ relative to VSMOW reference water and normalized on a scale such that SLAP reference water is −55.5 ‰ (Coplen, 1994). International reference materials were analyzed with samples and reported data were normalized in accordance with Böhlke and Coplen (1995) as described in Table 1. Two-sigma uncertainty for N isotopic results in samples with NO_3^- concentrations >0.06 mg/L as N was ±0.5 ‰ while samples with concentrations <0.06 mg/L as N was ±1 ‰.

3.6. Excess N_2 calculation

As denitrification occurs, excess N_2 is produced. Fig. 2A shows Ar and N_2 concentrations in groundwater samples along the expected concentrations from air saturated water between 5 and 25 °C (Weiss, 1970) at the mean elevation of sample collection (1651 m; Weiss, 1970). Samples that fall to the right of the line either contain excess air or excess N_2. As denitrification is an anoxic process, excess N_2 from denitrification is more likely at sites with low O_2 concentrations (Böhlke, 2002).

To estimate the amount of excess N_2 produced through denitrification the USGS Reston Groundwater Dating Laboratory Ar-N_2 workbook (https://water.usgs.gov/lab/dissolved-gas/) is used. Briefly, excess N_2 is estimated by using the concentrations of N_2 and Ar, their solubility in water at the likely recharge elevation (assumed to be the mean elevation of sample sites; Weiss, 1970), atmospheric pressure and the likely recharge temperature. The method assumes that the only source of Ar is the atmosphere, the only sources of N_2 are the atmosphere and denitrification, and excess air is not fractionated. It is further assumed that all samples were recharged at the same temperature but with varying amounts of excess air. For the assumed groundwater recharge temperature, the apparent recharge temperature 17 °C observed in Fig. 2A is used. For this analysis, only sites with O_2 concentrations <4 mg/L are considered.

The original NO_3^- concentrations prior to denitrification are then calculated by mass balance by Eq. (1):

$$[NO_3]^\circ = [NO_3] + 2[N_{2,denit}] \quad (1)$$

where $[NO_3]^\circ$ is the initial NO_3^- concentration (in molar units), $[NO_3]$ is the measured NO_3^- concentration and $N_{2,denit}$ is the estimated excess N_2. Reaction progress f (Table S6) was estimated by Eq. (2):

$$f = \frac{2[N_{2,1denit}]}{[NO_3]^\circ} \quad (2)$$

Initial $\delta^{15}N[NO_3]^\circ$ values were calculated to determine the original isotopic composition of sites prior to any denitrification that may have occurred following recharge. At sites where denitrification was suspected, calculations detailed in Green et al. (2008) were used to determine $\delta^{15}N[NO_3]^\circ$.

Carbon isotope analysis can help elucidate what denitrification pathway is occurring. Both oxic respiration (Eq. (3)) and heterotrophic denitrification (Eq. (4)) result in the production of bicarbonate (HCO_3^-).

$$O_2 + 0.5C_2H_3O_2^- \rightarrow 0.5H^+ + HCO_3^- \quad (3)$$

$$0.6H^+ + 0.8NO_3^- + 0.5C_2H_3O_2^- \rightarrow 0.4N_2 + HCO_3^- + 0.2H_2O \quad (4)$$

Hence, if NO_3^- reduction is occurring along with oxidation of organic material, then HCO_3^- and NO_3^- concentrations should be impacted along with C and N isotopes. The oxidation of organic material to inorganic carbon will produce very negative $\delta^{13}C$ values in dissolved inorganic carbon (DIC) whereas the dissolution of carbonate minerals will lead to near zero $\delta^{13}C$ values in DIC (Nikolenko et al., 2018). By contrast, autotrophic denitrification, uses zero-valent iron, ferrous iron, elemental sulfur or reduced sulfur compounds such as pyrite as an electron donor.

3.7. Carbon isotopes and ^3H analyses

Seventeen sites were selected for ^{14}C and $\delta^{13}C$ analysis (Tables 1 and S7) of DIC and ^3H. Samples for carbon isotopes were collected using a 1-L plastic coated glass bottle fitted with a polyseal cone cap. Bottles were filled from the bottom allowing bottles to overflow three sample volumes with filtered water (0.45 μm) and then capped immediately with no head space. Bottle tops were additionally sealed with electrical tape before being chilled. Samples were chilled, stored in the dark and analyzed within three months by accelerator mass spectrometry at the National Ocean Sciences Accelerator Mass Spectrometry (NOSAMS) facility at Woods Hole Oceanographic Institution (https://www2.whoi.edu/site/nosams/). The percent modern ^{14}C (PMC) is the deviation of the $^{14}C/^{12}C$ ratio of a sample from modern as defined as 95 % of radiocarbon concentration in AD 1950 of NBS Oxalic Acid (SRM 4990B, OX-1) and then normalized to $\delta^{13}C_{VPDB} = -19$

Fig. 1. Nitrate (NO_3) concentrations in water of sites sampled across the field area. Top map shows closeup of Kirtland Air Force Base (KAFB) while bottom map shows locations of sites outside of KAFB. Also shown is the approximate location of a perched aquifer layer and the 500-year (yr) floodplain of Tijeras Arroyo and potential anthropogenic NO_3 sources. Base map image is the intellectual property of Esri and is used herein under license. Copyright © 2020 Esri and its licensors. All rights reserved.

Table 1
Contaminants of emerging concern (CEC) are listed as number of detected compounds. Cl^-/Br^- and NO_3^-/Cl^- ratios are by mass. The regional and perched groundwater system (PGWS) are in aquifers of the Santa Fe Group. Data are available from the USGS National Water Information System (U. S. Geological Survey, 2022). Field blank concentrations were below the method detection limit while blank isotope results were not analyzed. Cells with no values represent sites with no corresponding sample. Nitrate isotopic data were normalized to be consistent with assumed values for reference materials USGS34 (δ15N = −1.8 ‰ and δ18O = −27.9 ‰) and USGS32 (δ15N = +180 ‰ and δ18O = +25.7 ‰; Böhlke et al., 2003).

Key results from groundwater samples

Site name	NO_3-N	Cl/Br	NO_3-N/Cl	CEC	^3H	$\delta^{15}N$ [NO_3]	$\delta^{18}O$ [NO_3]	$\delta^{15}N$ [N_2]	$\delta^{13}C$ [DIC]	^{14}C [DIC]	Water zone
	mg/L			n	pCi/L	‰	‰	‰	‰	PMC	
Abandoned Chical	13.5	130	0.5	1	16.2	10.1	9.30	−0.83	−12.6	105	Regional
ASL PD Well	1.90	70	0.1	0				0.59			Unknown
EGC-01	9.86	221	0.2	4		10.0	−4.0	0.58			Granite
EGC-17	0.455	352	0.0	2		15.1	1.6				Granite
IP1	1.52	88	0.1	1	<1	6.6	−0.2	0.64	−3.61	25	Regional
IP2	3.69	84	0.2	0		6.5	0.1	0.68			Regional
KAFB-0311	8.41	76	0.4	1		5.5	3.4	0.84			Regional
KAFB-0315	6.17	77	0.1	0		6.0	1.3	0.89			Regional
KAFB-0510	3.03	126	0.3	0	<1	5.7	3.3	0.76	−7.92	52	Regional
KAFB-0514	34.4	63	2.2	3	2.13	5.6	4.6	0.86	−8.74	52	Regional
KAFB-0516	6.97	122	0.5	1	<1	5.6	4.6	0.90	−7.87	48	Regional
KAFB-0517	2.46	172	0.2	6	<1	6.0	4.9	0.77	−7.27	48	Regional
KAFB-0518	6.79	94	0.9	3		6.0	6.0	0.83			Regional
KAFB-0525	14.4	67	0.8	1	<1	5.6	4.7	0.71	−8.23	55	Regional
KAFB-0615	7.49	77	0.1	8	<1	6.0	2.1	0.98	−5.45	29	Granite
KAFB-0618	6.51	68	0.8	1		6.2	4.1	0.84			Regional
KAFB-0619	9.82	62	0.8	1		6.2	3.0	0.94			PGWS
KAFB-0621	12.4	73	0.3	0		5.9	4.5	0.95			Regional
KAFB-0623	55.9	58	2.1	1		5.5	5.8	0.69			PGWS
KAFB-0624	24.4	69	0.9	4	<1	5.8	6.0	1.16	−5.32	25	Regional
KAFB-0901	3.85	78	0.1	1	<1				−7.92	60	Regional
KAFB-0903	4.75	151	0.3	0	21.2	4.3	−0.4	0.63	−6	76	Regional
KAFB-0904	26.2	61	1.8	3		5.8	4.6				Regional
KAFB-106009	10.2	76	0.03	10	<1	15.8	5.8	−0.60	−21.5	15	Regional
KAFB-6241	6.37	68	0.7	0	<1	5.3	1.2	0.80	−7.04	15	Regional
Montessa Site	0.499	243	0.0	0		5.9	3.9	0.74			Regional
MP1W-01	120	110	1.0	1		6.8	5.4	1.10			Regional
MVMW-B1	11.6	159	0.3	2		9.7	5.4	1.66			Regional
RIMW-01S	229	89	1.4	2		7.1	5.0	1.41			Regional
RIMW-03S	15.1	222	0.2	2		10.3	−0.8	0.57			Regional
RIMW-06S	113	46	3.9	3		6.2	6.6	0.82			Regional
RWP1	68.9	53	1.8	0		5.8	5.5				Regional
RWP19	0.046	351	0.001	0		16.2	5.2	0.89			Regional
RWP28	1.58			0		4.9	1.4	0.63			Regional
ST105MW003	3.08	142	0.4	0	<1	6.1	6.2	0.57	−7.09	56	Regional
ST105MW006	70.2	60	2.0	1		5.6	5.5	0.65			PGWS
ST105MW009	8.90	70	0.1	1		6.5	2.6	0.92			Regional
ST105MW015	9.06	71	0.3	0		6.4	5.0	2.40			Regional
ST105MW017	10.5	70	0.5	0		5.8	3.9	0.91			Regional
ST105MW020	5.15	89	0.1	1		7.8	0.6	0.82			PGWS
ST105MW024	1.97	77	0.0	0		6.4	3.0	1.26			Regional
TA2-W-19	10.5	78	0.2	1		6.1	3.7	0.61			PGWS
TA2-W-28	16.0	68	0.5	0	<1	6.0	4.6	0.75	−6.23	18	PGWS
TJA-2	11.0	78	0.2	2		6.2	4.0	0.85			PGWS
TJA-3	2.66	83	0.2	0		5.8	2.5	0.85			Regional
TJA-4	29.7	64	1.3	1		5.4	5.5	0.82			Merging zone
TJA-5	24.7	64	1.0	1		5.9	6.3	0.66			PGWS
TJA-7	21.6	60	0.9	1		5.9	5.5	0.75			PGWS
UES-4	2.61	84	0.1	0	<1	4.5	0.9	0.51	−7.62	62	Regional

Key results from surface water samples

Site name	NO_3-N	Cl/Br	NO_3-N/Cl	CEC	^3H	$\delta^{15}N$ [NO_3]	$\delta^{18}O$ [NO_3]	$\delta^{13}C$ [DIC]	^{14}C [DIC]	Water zone
	mg/L			n	pCi/L	‰	‰	‰	PMC[a]	
Carlito Spring	0.197	56	0.1	3	6.2	5.0	−5.9	−11	70	Spring
Hell Tank Spring	2.62			0		7.7	4.1			Spring
Hubbell Spring	0.556			1		6.9	0.8			Spring
Carlito Stream	<0.04	53		3						Stream
Tijeras Creek	0.07	414	0.0004	4		12.9	3.1			Stream
Tijeras Arroyo 1	<0.040	29		6						Ephemeral stream
Tijeras Arroyo 2	3.30	74	1.1	32		5.3	12.3			Ephemeral stream
Tijeras Arroyo 3	4.73	83	1.1	24		5.4	9.9			Ephemeral stream
Tijeras Arroyo 4	4.82	125	0.8	21		4.7	8.2			Ephemeral stream

[a] ^{14}C [DIC] PMC results have been de-normalized according to Han and Plummer (2016).

(Olsson, 1970). Reported uncertainty of PMC values encompasses the counting errors from 10 separate measurements of the $^{14}C/^{12}C$ ratio measured on each individual sample. As recommended by (Han et al., 2012; Han and Plummer, 2016), ^{14}C data have been de-normalized from laboratory reported values in order to better account for water-rock interactions during age calculations. Counting errors of ^{14}C measurements were <0.2 PMC (Table S7). Groundwater ages were estimated using ^{14}C and a method developed by Han and Plummer (2016). Details of this work are described in S.7.

Samples for ^{3}H analyses were unfiltered and collected in unrinsed 1-L polyethylene bottles filled without overflow. Analyses were completed at the Tritium Laboratory at the University of Miami using gas proportional counting (https://tritium.rsmas.miami.edu/). ^{3}H was measured through internal gas proportional counting of H_2 gas made from the water sample. Prior to analyses, samples underwent an electrolytic enrichment step during which ^{3}H concentrations are increased through volume reduction. Accuracy was 0.3 pCi/L or 3.5 %, whichever was greater.

4. Results

Key results from the study are presented in Table 1; all data are available in Table S3 and in the USGS National Water Information System database (U. S. Geological Survey, 2022) by using the site identifiers presented in Table S1.

4.1. Ion concentrations and $\delta^{15}N$ $[NO_3]$, $\delta^{18}O$ $[NO_3]$, and $\delta^{15}N$ $[N_2]$ results

Results of N species as well as Cl^- and Br^- concentrations are shown in Table S2. Dissolved NO_3^- concentrations varied between below the detection limit to 229 mg/L (NO_3-N) with a mean of 19.4 mg/L (n = 56). Of the groundwater sites sampled (n = 49), 22 concentrations exceeded the EPA maximum contaminant level (MCL) for NO_3^- (>10 mg/L NO_3-N).

Reduced species of N including ON, ammonia and ammonium ($NH_3$and NH_4^+) and nitrite (NO_2^-) were detected at 12 sites. On KAFB, sites with reduced N species were in the northeast side of the field area (ST105MW015, ST105MW017, and KAFB-0901) and KAFB-106009 which is situated beneath a recent accidental sewer line release (Fig. 1). Table 1 has results from $\delta^{15}N$ $[NO_3]$, $\delta^{18}O$ $[NO_3]$, and $\delta^{15}N$ $[N_2]$ analyses. $\delta^{15}N[NO_3]$ varied from 4.3 ‰ to 16.2 ‰ (mean = 6.9 ‰, n = 54), $\delta^{18}O[NO_3]$ varied from −5.9 ‰ to 12.3 ‰ (mean = 3.8 ‰, n = 54), and $\delta^{15}N[N_2]$ varied between −0.83 ‰ and 2.40 ‰ (mean = 0.79 ‰, n = 45), respectively.

4.2. Estimated denitrification, initial $[NO_3]^\circ$, and initial $\delta^{15}N$ $[NO_3]^\circ$

Calculated results of excess N_2 from denitrification, NO_3°, HCO_3^- produced through denitrification, f, and $\delta^{15}N[NO_3]^\circ$ are summarized in Table S6. Five sites had excess N_2 likely from denitrification (KAFB-106009, MVMW-B-1, ST105MW015, MP1W-01, RIMW-01S; Fig. 2A; Table S6). The highest f value (31 %) was observed at KAFB-106009 where 4.5 mg/L of excess N_2 was produced and $[NO_3]^\circ$ and $\delta^{15}N$ $[NO_3]^\circ$ were estimated to be 14.7 mg/L and 9.5 ‰, respectively (compared to the measured NO_3-N and $\delta^{15}N$ $[NO_3]$ values of 10.2 and 15.8 ‰, respectively). ST105MW015 also had a relatively high calculated f value of 28 %. At this site, estimated $[NO_3]^\circ$ was 12.6 mg/L NO_3-N, $\delta^{15}N[NO_3]^\circ$ was 6.5 ‰ and 3.5 mg/L of excess N_2 was produced. As the measured NO_3^- concentrations were 9.06 mg/L NO_3-N at ST105MW015, denitrification appears to have lowered NO_3^- concentrations to below the EPA's MCL.

To test the reality of excess N_2 calculations, excess N_2 was plotted against O_2 concentration; higher excess N_2 should correspond to lower O_2 concentrations and higher $\delta^{15}N$ $[NO_3]$ values. Fig. S2 shows that generally this is the case with sites with low O_2 having elevated $\delta^{15}N$ $[NO_3]$ and excess N_2. Sites with higher O_2 concentrations (>4 mg/L) likely have not undergone any denitrification which explains the scatter around zero excess N_2 in Fig. S2 at high O_2 sites. The standard deviation of excess N_2 at sites with >4 mg/L O_2 (Fig. S2) was used as an estimate of uncertainty. Using this method, excess N_2 uncertainty was ±1.4 mg/L.

A trend was observed of decreasing $\delta^{13}C$[DIC] with increasing HCO_3^- concentrations (Fig. S3) that is consistent with heterotrophic denitrification. Additionally, NO_3^- reduction will cause the fractionation of $\delta^{15}N$. Fig. S3 shows a general increase in both HCO_3^- and $\delta^{15}N[NO_3]$. Assuming the reduction of 0.3 mmol of O_2, 0.3 mmol (18.5 mg/L) of HCO_3^- will be produced through Eq. 3. Using the estimated excess N_2 (Table S6) for sites with <0.14 mmol/L (5 mg/L) O_2, an additional 1.7–53 mg/L HCO_3^- was produced according to Eq. (4). Table S6 shows the estimated HCO_3^- produced from NO_3^- and O_2 reduction. This is enough to explain the increase in HCO_3^- with increasing $\delta^{15}N$ shown in Fig. S3.

4.3. Contaminants of emerging concern results

In total, 44 different CECs were detected in groundwater and surface water sites. At least one CEC (including artificial sweeteners) was found in 67 % of sites sampled for these constituents. The number of different sites each CEC was detected at is listed in Table S8. The surface water site Tijeras Arroyo had the highest number of detectable CEC with between 5 and 30 detected in each sampling event. CEC were also found in all other surface water sampling sites. Of the 38 sites where both WWI and artificial sweeteners were measured, only five had no detections. These included KAFB-0315 (northeast KAFB), KAFB-0510 (northwest KAFB), KAFB-0621 (northeast KAFB), KAFB-6241 (southeast KAFB), and TJA-3 (central KAFB). Exceedances included four sites with tetrachloroethylene over the EPA's maximum contaminant level (MCL) goal (0 μg/L; EPA, 2021) located in both the perched aquifer on KAFB (KAFB-0623, ST105MW006) and in the Mountain View community (MP1W-01, RIMW-01S). Additionally, benzo(*a*)pyrene was found in the surface water Tijeras Arroyo above the EPA MCL (0.2 μg/L; EPA, 2021).

Of all sites sampled, 21 had measurable detections of artificial sweeteners (Table S9 and Fig. S4). Neotame was the most detected sweetener (n = 12) followed by saccharin (n = 4), acesulfame-K (n = 2), aspartame (n = 1), and sucralose (n = 0). Concentrations ranged from 0.3 to 11 ng/L for neotame, 19 to 630 ng/L for saccharin, 840 to 11,000 for acesulfame-K, and 1.6 ng/L for aspartame.

Pharmaceuticals were generally not detected in groundwater with the exception of a domestic well in Carnuel that contained Fluconazole (antifungal) and Carbamazepine (anticonvulsant). In the Tijeras Arroyo surface water site, Metformin (anti-diabetic) and Acetaminophen (pain killer) were detected along with the human-use products cotinine (a byproduct of nicotine), nicotine, and caffeine.

4.4. Dissolved gas results

Four sites had detectable CH_4 (Abandoned Chical, ST105MW015, KAFB-0619; and KAFB-106009) which varied between 0.0026 and 9.7 mg/L (mean 2.4, n = 4; Table S5). Dissolved N_2 concentrations varied between 12.7 and 29.9 mg/L (mean = 16, n = 47). Out of the 47 sites sampled, five sites had low O_2 concentrations (<2 mg/L; KAFB-106009, Abandoned Chical, RWP19, MWMW-B1, KAFB-0618). Dissolved Ar varied between 0.4 and 0.8 mg/L with a mean of 0.5 mg/L (n = 47).

4.5. Carbon isotopes and ^{3}H results

Carbon isotope results are displayed on Tables 1 and S7. $\delta^{13}C$ in groundwaters varied between −21.5 and −3.61 ‰ while the median $\delta^{13}C$ value was −7.62 ‰ (n = 17; Table 1). ^{14}C results varied from 15 to 105 PMC with a median of 52 (n = 17). Detailed analysis of ^{14}C isotopes (S.7) show that no sites sampled had datable pre-modern groundwater. However, low ^{14}C values in water from some sites are likely components of recent recharge and intermediate waters where old groundwater is mixing with relatively recent recharge (S.7). Modern ^{3}H was defined as sites containing concentrations >1 pCi/L ^{3}H while ^{3}H dead is here defined as sites with <1 pCi/L ^{3}H. Of the 17 sites analyzed for ^{3}H content, only four (Abandoned Chical, Carlito Spring, KAFB-0514, and KAFB-0903) had ^{3}H >

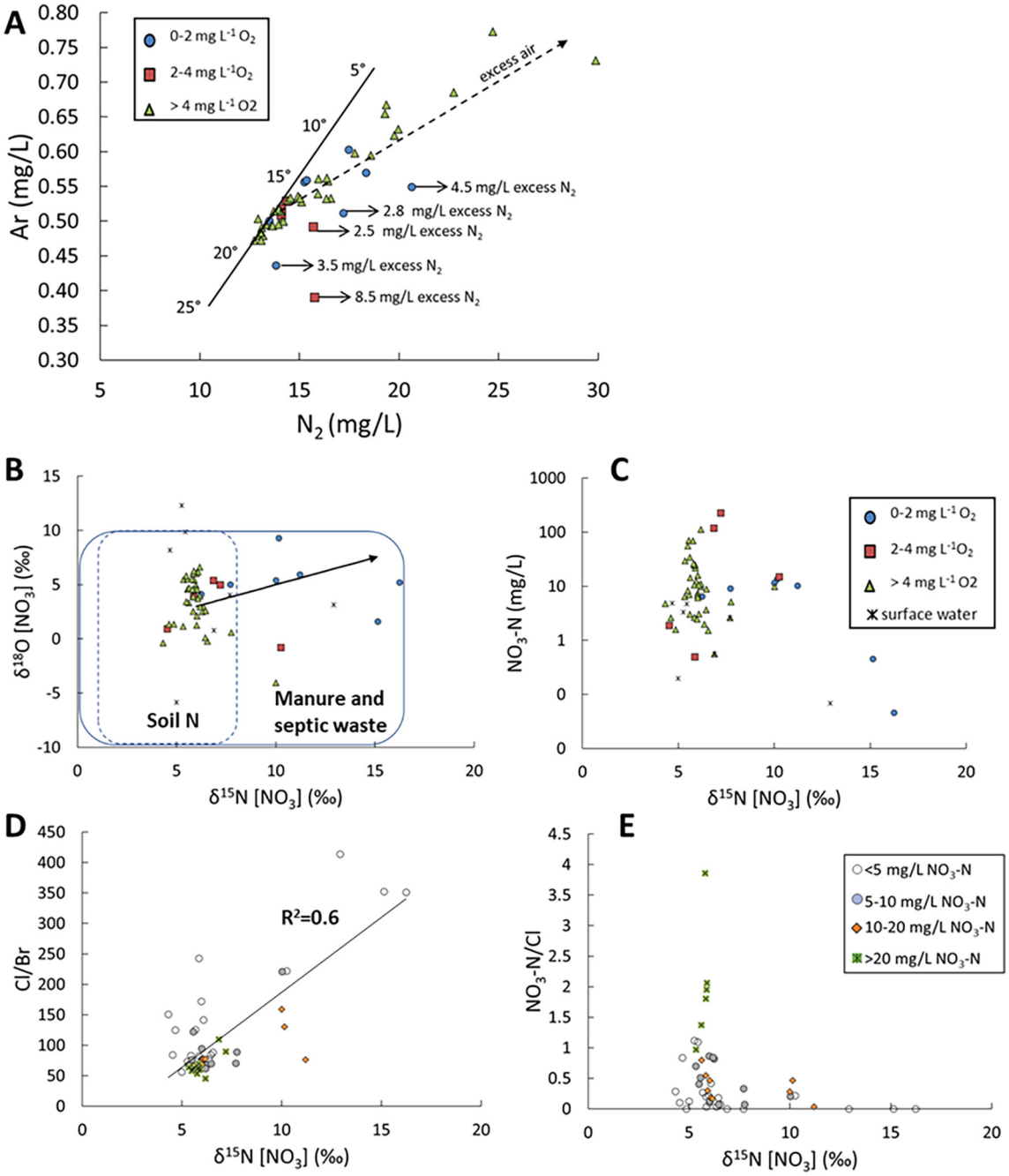

Fig. 2. Plot A shows Ar and N_2 concentrations of samples and their corresponding O_2 content. Also shown is air-saturated water (solid line) in equilibrium with different temperatures at the mean elevation of collected samples (1651 m). Additionally, arrows are plotted showing the pathway of groundwater mixing with excess air and estimated excess N_2 of samples where NO_3^- reduction was suspected. Plot B shows the relationship between and $\delta^{18}O[NO_3]$ vs. $\delta^{15}N[NO_3]$ isotopes and dissolved oxygen (O_2) concentrations. Eight sites had a composition consistent with a manure or septic waste source. The arrow shows the isotopic progression of denitrification (slope is generally between 1:1 and 1:2). Plot C shows that the highest NO_3^- concentrations were not associated with a clear manure or septic source. Plot D shows a correlation between Cl^-/Br^- mass ratios and $\delta^{15}N$ $[NO_3]$ suggesting wastewater is partially driving $\delta^{15}N[NO_3]$ values. Plot E shows that elevated the NO_3^-/Cl^- mass ratio—associated with vadose zone NO_3^- reservoirs—is not correlated to high $\delta^{15}N$ $[NO_3]$. In all figures, at sites where excess N_2 was detected, initial $\delta^{15}N[NO_3]^\circ$ values are used.

1 pCi/L and therefore may be considered influenced by modern ^3H. Of these modern groundwaters, all had ^{14}C values >50 PMC (Table 1).

5. Discussion

5.1. Differentiating natural and anthropogenic NO_3^- using major ions

In the study area, Cl^-/Br^- ratios (by mass) varied between 29 and 414 (Table 1; mean = 108, n = 54). Fig. 3, showing Cl^-/Br^- ratios against Cl^- concentrations, indicates the hypothetical mixing line (dashed line) between non-impacted groundwaters and sewer or septic wastewater sources. The highest Cl^-/Br^- ratio was observed in Tijeras Creek (Fig. 3), a small perennial creek that turns into Tijeras Arroyo downstream at lower elevations prior to entering KAFB (Fig. 4). The Tijeras Creek site is in the community of Carnuel (far east in Fig. 4), which has long been impacted by elevated NO_3^- in groundwater likely due to domestic septic leach fields (Bartolino et al., 2005). The EGC sites 1 and 17 are also in Carnuel and similarly have elevated Cl^-/Br^- ratios as well as CEC detections (artificial

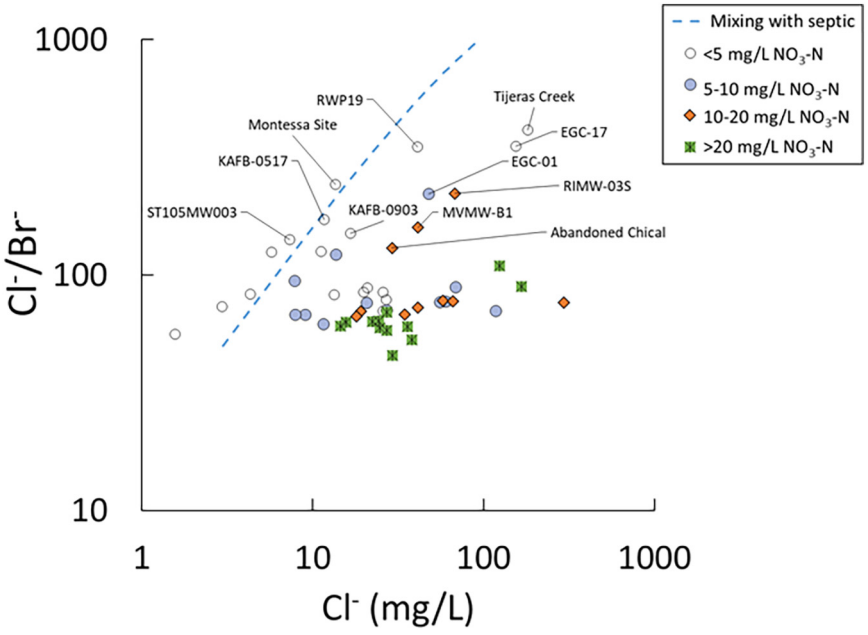

Fig. 3. Chloride (Cl^-)/bromide (Br^-) mass ratios by mass versus Cl^- concentrations. Dashed lines show the mixing pathway of dilute groundwater with a hypothetical septic or sewer wastewater with Cl^- and Br^- concentrations of 126 Cl^- mg/L and 0.21 mg/L respectively (Katz et al., 2011). Labeled sites have elevated Cl^-/Br^- ratios potentially indicating influence from septic or sewer wastewater sources.

sweeteners neotame and acesulfame-K and pharmaceuticals fluconazole and carbamazepine). These high Cl^-/Br^- ratios and CECs are likely the result of septic contaminated groundwater that discharges to Tijeras Creek.

On KAFB, sites with relatively high Cl^-/Br^- ratios include KAFB-0516, KAFB-0517, KAFB-0510, KAFB-0903, and ST105MW003. Except for KAFB-0510, all these sites are located on the floodplain of Tijeras Arroyo. Pulling from the regional aquifer, KAFB-0516, KAFB-0517, and ST105MW003 are located near past accidental sewer line releases that occurred in 1994, 2003, and 2013 (Copland, 2019) on the western margins of the base while KAFB-0903 is located upstream on the eastern edge of KAFB near former landfills and housing development (Figs. 1 and 4). Downstream, the Montessa Site is located ~1 km west of KAFB in the Tijeras Arroyo floodplain (Figs. 1 and 4). This site may be impacted by a nearby (<0.25 km) former landfill used for sludge disposal of Albuquerque's wastewater treatment facility (Agency, 1981). Other sites with elevated Cl^-/Br^- ratios include MVMW-B1 in the Mountain Valley neighborhood located downstream (west) of KAFB in the Tijeras Arroyo floodplain. Other sites with relatively high Cl^-/Br^- ratios include the Abandoned Chical well and RWP19 on Isleta Pueblo (Fig. 3).

Based on Cl^-/Br^- ratios, wastewater appears to be reaching groundwater in parts of the field area including beneath Tijeras Arroyo on KAFB (Fig. 4). However, the recently discovered large subsoil NO_3^- reservoir in the floodplain of Tijeras Arroyo on KAFB clearly plays a major role in NO_3^- chemistry (Linhoff and Lunzer, 2021). Notably, the highest groundwater NO_3^- concentrations were not associated with high (>100) Cl^-/Br^- ratios but instead, very high NO_3^- (>20 mg/L NO_3-N) corresponded to high NO_3^-/Cl^- (>1.5) and low Cl^-/Br^- (<65) ratios (Fig. 5). These sites were all located on the floodplain of Tijeras Arroyo except for RWP1, which is in the floodplain of Hell Canyon Arroyo (a large arroyo ~14 km to the south of KAFB; Figs. 1 and 4). Subsoil porewater in the floodplain of Tijeras Arroyo is associated with very low porewater Cl^-/Br^- (15 to 83, mean = 41) and very high NO_3^-/Cl^- (0.1 to 30, mean = 6.6) ratios (Linhoff and Lunzer, 2021). Consequently, at this field site, NO_3^- in groundwater sourced from the vadose zone NO_3^- should have low Cl^-/Br^- and high NO_3^-/Cl^- ratios in contrast with anthropogenic NO_3^- sources. For example, RIM-06S, located in the Tijeras Arroyo floodplain (Fig. 1), had a clear subsoil NO_3^- source based on major element ratios with exceptionally high NO_3^- concentrations (113 mg/L NO_3-N), low Cl^-/Br^- (46) and high NO_3^-/Cl^- (3.9) ratios. It did however contain three CECs which may have been sourced from a highway 50 m away. Based on this evidence, the presence of CECs alone cannot be used to differentiate between NO_3^- sourced from arid region subsoil NO_3^- reservoirs and anthropogenic wastewater.

Linhoff and Lunzer (2021) infer that the arroyo floodplain subsoil NO_3^- reservoirs may be flushed to the aquifer through arroyo channel migration over the floodplain. This flushing could also occur through large sewer line releases which would act to saturate the subsoil and mobilize subsoil NO_3^- to the aquifer. For example, site KAFB-0514 is located directly under and adjacent to a major accidental sewer line releases in 1994, 2003, and 2013 (Copland, 2019) though it has low Cl^-/Br^- (63) and high NO_3^-/Cl^- (2) ratios along with elevated NO_3^- (34.4 mg/L NO_3-N) and three CEC detections; these elemental ratios suggest subsoil NO_3^- constitutes the bulk of the NO_3^- source while CECs indicate a limited wastewater contribution.

If the subsoil NO_3^- in the arroyo floodplain is a major NO_3^- source to the aquifer, this influence should be seen in other major ion ratios. In the arroyo floodplain, Linhoff and Lunzer (2021) found that subsoil porewater mass ratios of NO_3^-/Cl^- and Cl^-/Br^- were similar to local precipitation. If ratios of Ca^{2+}, Mg^{2+}, and Na^+ in subsoil porewaters are also similar to local precipitation, these cations may help trace the NO_3^- source. There is a correlation between the ratios of TN/Cl^-, TN/Na^+, TN/Ca^{2+}, and TN/Mg^{2+} in groundwater in the arroyo floodplain and ratios in the local precipitation (Fig. 6). If the major ion ratios in precipitation match those in the subsoil porewaters—as was observed for NO_3^-, Cl^-, and Br^- in Linhoff and Lunzer (2021)—the correlations seen in Fig. 6 likely indicate that the bulk of the high NO_3^- groundwater concentrations beneath the arroyo floodplain are derived from the subsoils. Altogether, Figs. 3, 5, and 6 suggest that while much of the NO_3^- contamination in the region is from both anthropogenic and natural sources, the highest NO_3^- groundwater concentrations are of natural origin. Sites that have high NO_3^- but neither elevated Cl^-/Br^- nor NO_3^-/Cl^- ratios (Fig. 5) cannot be clearly differentiated using these elemental ratios and may contain a mixture of both natural and anthropogenic NO_3^- sources; N isotopes, CECs, and C isotopes provide clarification for many of these sites as described below.

If naturally occurring vadose zone NO_3^- is a major source to the aquifer, mass balance of the source must be considered. Assuming a saturated aquifer thickness of 30 m and a porosity of 0.2, and complete mixing over this depth, as noted in Linhoff and Lunzer (2021), flushing all observed subsoil

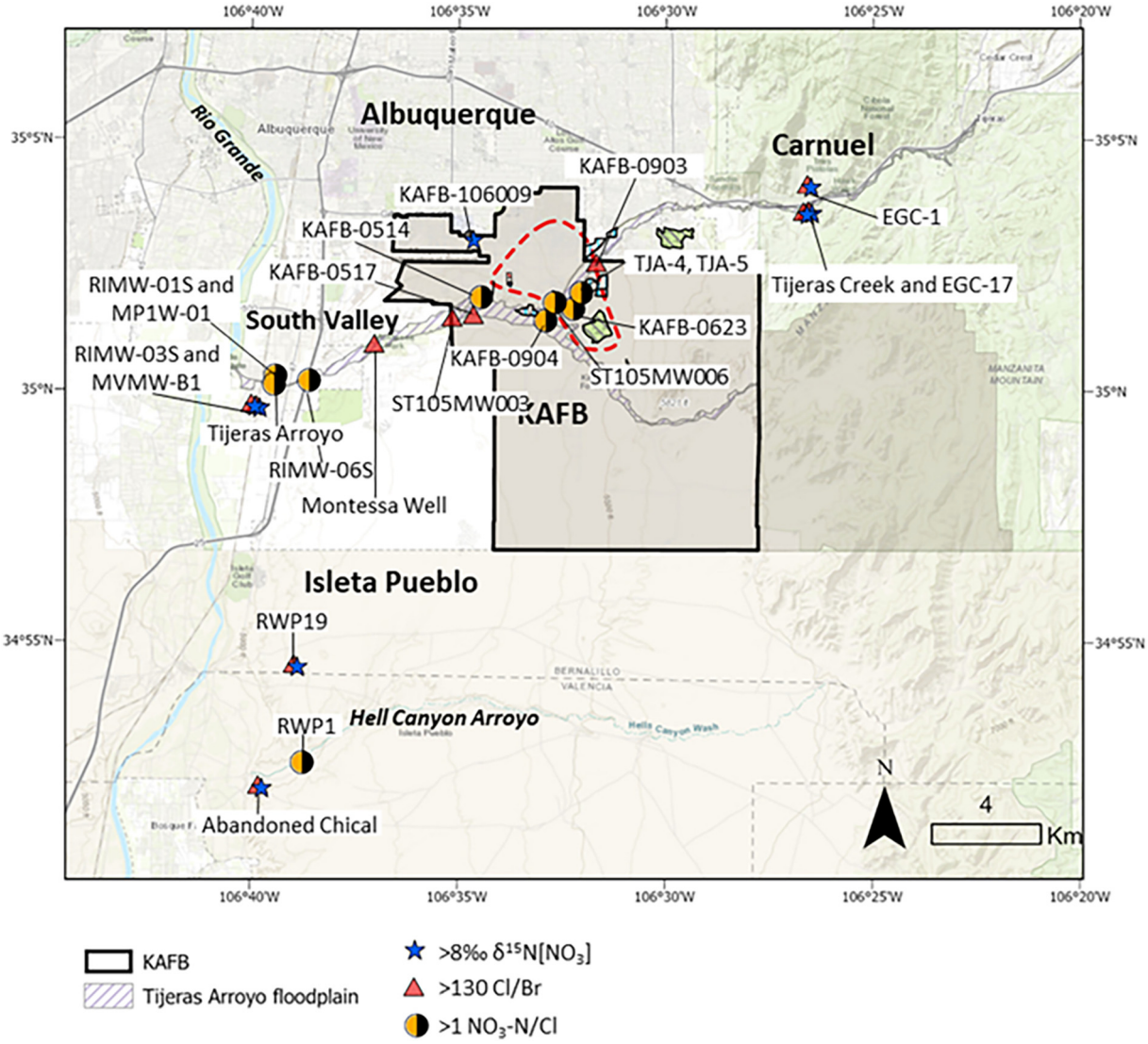

Fig. 4. Locations of samples collected with elevated NO_3^-/Cl^- or Cl^-/Br^- ratios as well as sites with >8 $\delta^{15}N$ $[NO_3]$. Base map image is the intellectual property of Esri and is used herein under license. Copyright © 2020 Esri and its licensors. All rights reserved.

NO_3^- (10,000 to 38,000 kg NO_3-N/ha) to the aquifer would result in groundwater NO_3^- concentrations between 167 and 633 mg/L NO_3-N. However, hydraulic conductivity in the Upper Santa Fe Group aquifer is likely between 0.5 and 12 m/day (Kernodle, 1998), hence flushing subsoil NO_3^- to the aquifer through the migration of the arroyo channel over the floodplain or through land use changes (such as irrigation, septic leach fields, leaky infrastructure, etc.) would result in pulses of high NO_3^- that would soon be diluted. For example, accidental sewer line releases on KAFB have likely provided a mechanism for flushing subsoil NO_3^- to the aquifer. After multiple sewer line releases, time series sampling at KAFB-0514, KAFB-0516, and KAFB-0517 revealed pulses of elevated NO_3^- (60 to 70 mg/L NO_3-N) with correspondingly high NO_3^-/Cl^- ratios (2 to 3). These were followed by high Cl^-/Br^- ratios (>130) and decreasing NO_3^- concentrations (Fig. S5). This observation suggests the sewer line releases acted to flush subsoil NO_3^- to the aquifer as also suggested by the presence of CECs (Table 1). Due to the very large size of the subsoil NO_3^- reservoir mobilized, the groundwater chemistry following the sewer line releases was dominated by the natural (high NO_3^-/Cl^- ratios) rather than the anthropogenic signal (high Cl^-/Br^-). Once the subsoil reservoir was exhausted, the anthropogenic NO_3^- signal was then observed. This is discussed in more detail in S.8.1.

5.2. Nitrate fate

Anthropogenic N sources often contain reduced N species such as ON, NH_4^+, and NO_2^- though these can also be found naturally (Robertson and Cherry, 1992; Zhang et al., 2015). Dissolved ON in groundwater may be from forests and wetlands (Perakis and Hedin, 2002) or anthropogenic sources such as wastewater (Kroeger et al., 2006) and agricultural inputs (Lorite-Herrera et al., 2009). In this study, ON was detected at sites that contained other reduced N species and CEC detections as well as low O_2 (<2 mg/L), hence, an anthropogenic source for ON is likely (Tables S2 and S5). In addition, three of four sites with detectable CH_4 also contained reduced N species (Tables S2 and S5).

Water samples from eight sites contained elevated $\delta^{15}N[NO_3]$ indicative of NO_3^- largely sourced from human wastewater or manure ($\delta^{15}N$ $[NO_3]$ > 8 ‰; Figs. 2B, 4, and Table 1). Nitrate concentrations at these sites varied between 0.05 and 15.5 mg/L NO_3-N (Fig. 2C). At sites where denitrification had likely occurred in the aquifer (Table S6), NO_3^- source appropriation using NO_3^- isotopes (Fig. 2) was done using $\delta^{15}N[NO_3]^*$ instead of measured values to avoid assigning a wastewater source to groundwater that has naturally undergone denitrification in the aquifer. KAFB-106009 was the only site on KAFB that contained elevated $\delta^{15}N[NO_3]^*$

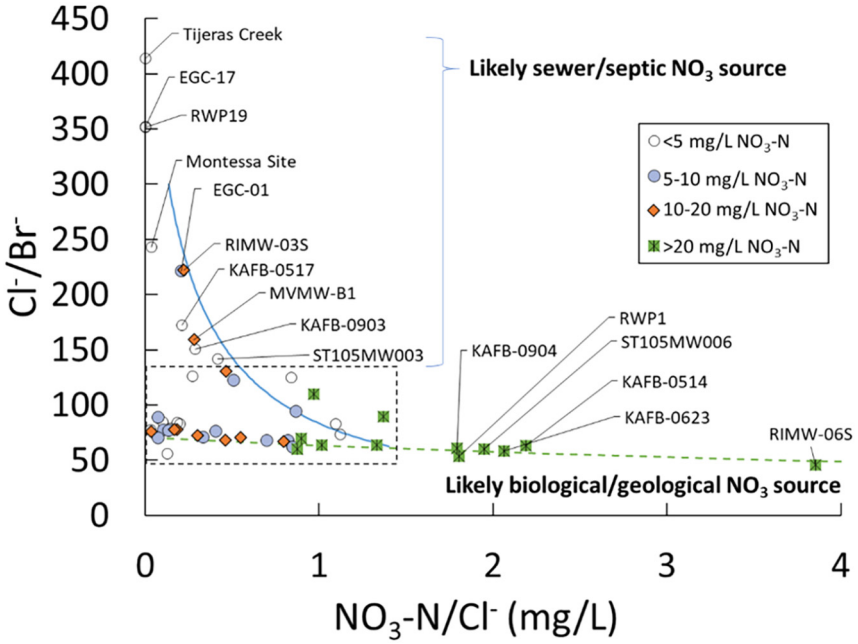

Fig. 5. Mass ratios of chloride (Cl^-)/bromide (Br^-), compared to nitrate (NO_3-N)/Cl^- ratios through the field area. A dashed line is shown for two end member mixing between a vadose zone biological/geological NO_3^- source (2000 mg/L NO_3-N, 200 mg/L Cl, and 6 mg/L Br; Linhoff and Lunzer (2021) and dilute groundwater. The solid mixing line shows the potential two end member mixing between a representative septic influenced groundwater (20 mg/L NO_3-N, 150 mg/L Cl, 0.5 mg/L Br; Katz et al., 2011) and a vadose zone biological/geological NO_3^- influenced groundwater (70 mg/L NO_3-N, 50 mg/L Cl, and 0.8 mg/L Br; Linhoff and Lunzer, 2021). The dashed box of mixed NO_3^- sources may show a blend of multiple NO_3^- sources and mixing pathways.

(11.2 ‰); this site is located next to a recent accidental sewer line release which is likely the NO_3^- source (Figs. 1 and 4). Other sites with elevated $\delta^{15}N[NO_3]$ were in Carnuel, Mountain View, and on Isleta Pueblo; these sites generally contained lower O_2 concentrations (<0.1–4 mg/L) likely because wastewater has low O_2 content (Taylor et al., 2003). Several surface water sites had relatively high $\delta^{18}O[NO_3]$ values ($\delta^{18}O[NO_3] > 9$ ‰; Fig. 2B) and $\delta^{15}N[NO_3]$ values near 5 ‰. This could indicate mixing with unaltered atmospheric NO_3^- deposition in surface waters.

The isotopic composition of the subsoil NO_3^- is unknown. Evaporite salts in Death Valley, USA have $\delta^{18}O[NO_3]$ values ~45 ‰, values high enough to argue for an atmospheric N source (Böhlke et al., 1997). NO_3^- accumulated in the subsoils of arroyo floodplains is likely derived from N in the arroyo channel stream water through evapoconcentration and the nitrification of reduced N species. $\delta^{18}O[NO_3]$ of the Tijeras Arroyo water varied between 8.2 ‰ to 12.3 ‰ (Table 1). During nitrification, two oxygens are derived from water ($\delta^{18}O[H_2O] = -25$ ‰ to +4) while one is from the atmosphere ($\delta^{18}O$ + 23 ‰; (Kendall, 1998). Hence, nitrification generally produces waters with $\delta^{18}O[NO_3]$ values between −10 ‰ and + 10 ‰. Further N cycling in the subsoils and oxygen exchange between NO_3^- and water will also produce NO_3^- isotopic results in the range of normal soil N (Kendall, 1998). Therefore, it is unlikely that NO_3^- derived from the subsoil vadose zone can be differentiated through the isotopes of NO_3^- in groundwater. As might be expected for a subsoil NO_3^- source, sites with highly elevated NO_3^- concentrations (16–229 mg/L NO_3-N) all had $\delta^{15}N[NO_3]$ and $\delta^{18}O$-NO_3 values in line with soil ON (Fig. 2B and C).

Elevated Cl^-/Br^- ratios in groundwater often correspond to human and animal wastewater sources (Davis et al., 1998; Panno et al., 2006). If >8 ‰ $\delta^{15}N[NO_3]$ values are indicative of inputs from septic waste, then increasing Cl^-/Br^- ratios should correspond to an increase in $\delta^{15}N[NO_3]$. Fig. 2D shows a correlation ($r^2 = 0.61$) between higher Cl^-/Br^- ratios and $\delta^{15}N[NO_3]$. If elevated NO_3^-/Cl^- ratios correspond to vadose zone NO_3^- at this field site (Linhoff and Lunzer, 2021), then high NO_3^-/Cl^- ratios should correspond to lower $\delta^{15}N[NO_3]$ values in line with soil N. This relationship is shown in Fig. 2E. The lower NO_3^-/Cl^- ratios with respect to higher $\delta^{15}N[NO_3]$ values could also be the result of denitrification. However, recalculating the NO_3^-/Cl^- ratios with the calculated $[NO_3]^\circ$ concentrations (Table S6) prior to denitrification results in only a very small shift in the NO_3^-/Cl^- ratios. For example, using the estimated $[NO_3]^\circ$ concentration (12.6 mg/L NO_3-N) for ST105MW015 instead of the measured NO_3^- (9.06 mg/L NO_3-N) value results in a NO_3^-/Cl^- ratio of 0.5 instead of 0.3.

5.3. Contaminants of emerging concern

Most CEC (WWI, pharmaceuticals, and artificial sweeteners) have been synthesized in the last century and do not occur naturally in the environment. Ideal CEC compounds for tracing wastewater are those that are present at sufficient concentrations in wastewater, persistent in the subsurface environment, and amenable to rapid and sensitive analysis (McCance et al., 2018). Detection of CEC in groundwater can be used as an indication of anthropogenic pollution sources and of recent recharge (Lee et al., 2019). CECs were found in nearly every part of the field area including the regional and perched aquifers on KAFB, rangeland on Isleta Pueblo south of KAFB, and the neighborhoods sampled east (Carnuel) and west (Mountain View) of KAFB (Table 1 and Fig. 1).

Like NO_3^- concentrations, groundwater sites with a greater depth to water tended to have fewer CECs (Fig. S5) indicating a surface source for both NO_3^- and CEC. All sites with no CEC detections were in wells with water levels >125 m below land surface. Surface waters had by far the highest number of CECs with 5 to 32 detections in the ephemeral stream Tijeras Arroyo. Past work on pharmaceuticals in groundwater has shown most frequent detections are in shallow wells with a young water component, fractured crystalline bedrock, in domestic wells, and in areas of mixed land use (Bexfield et al., 2019). That result was repeated in this study with shallower wells, wells screened in the fractured granite bedrock, and developed areas had the highest number of CEC detections which agreed with the findings of Bexfield et al. (2019). Pharmaceuticals were nearly absent throughout the field area possibly because of the depth of the water table and the short half-life of many of these compounds (Bexfield et al., 2019). Caffeine and acetaminophen have been proposed as specific molecular markers of wastewater (Tran et al., 2014), however, these chemicals were only measured in surface water samples from the

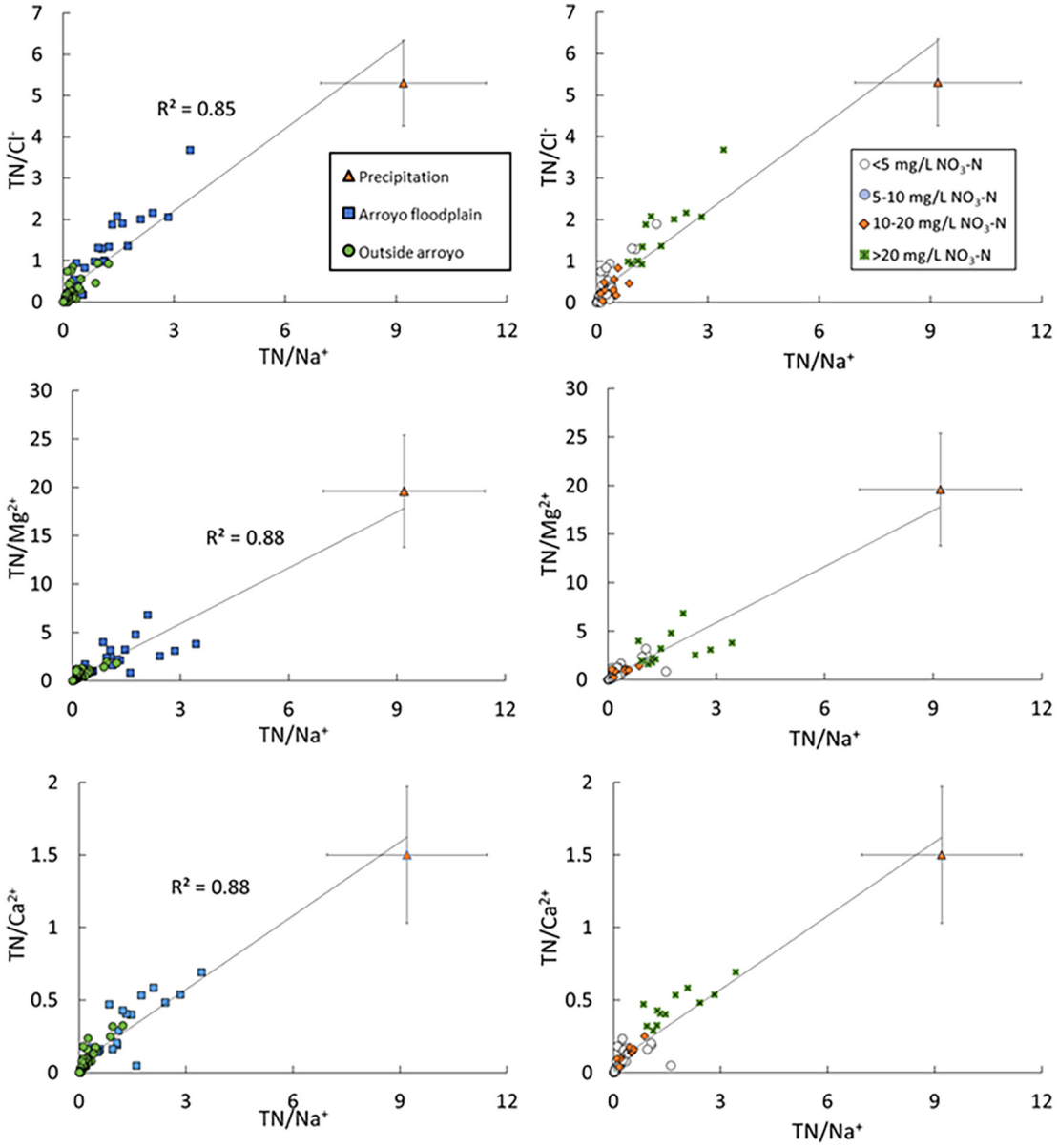

Fig. 6. Major ion mass ratios of sites outside and within the arroyo floodplain. All locations with elevated total nitrogen (TN)/sodium (Na) ratios are located in the arroyo floodplain. A correlation was found between these major ion ratios and precipitation. Precipitation marker represents the average precipitation of 37 years of data (1982—2018) while error bars represent 1σ uncertainty (National Atmospheric Deposition Program, 2022).

ephemeral stream Tijeras Arroyo and are likely less stable then compounds such as bisphenol A (BPA).

Excluding artificial sweeteners, the five most commonly detected CECs were BPA, diethyl phthalate (DEP; plasticizer and cosmetics), triphenyl phosphate (TPhP; flame retardant and plasticizer), N,N-diethyl-m-toluamide (DEET; insect repellent), and phenol (biodegradation product of aromatic hydrocarbons). These compounds are commonly found in wastewater, groundwater, and surface waters (Margot et al., 2015; Peng et al., 2014). BPA concentrations in wastewater are generally ~1 μg/L and an order of magnitude lower in wastewater treatment facility effluent and landfill leachate (Margot et al., 2015; Peng et al., 2014). In this study, BPA varied from 0.03 to 2.13 μg/L with the highest concentrations found in the surface water site, Tijeras Arroyo (0.18–2.13 μg/L), and KAFB-0615 (1.83 μg/L) located in the southeast portion of KAFB. BPA detections were confined to KAFB and the Mountain View neighborhood west of KAFB.

DEP and DEET are commonly associated with wastewater (Margot et al., 2015). DEP detections in groundwater were centered near recent accidental sewer line releases (KAFB-0514, 0516, 0517) and near the northeast side of KAFB near a residential area (KAFB-0624, ST105MW009). It was also detected in multiple samples from the Tijeras Arroyo surface water site west of KAFB. DEET was detected in the same areas but at fewer sites.

TPhP was detected at KAFB-0311, KAFB-0514, KAFB-0615, KAFB-0904, TA2-W-19, and TJA-7 on KAFB as well as at RIMW-06S west of KAFB. These detections largely center in the regional or perched aquifers around Tijeras Arroyo with the exception of KAFB-0615 and TA2-W-19. TPhP has been used extensively as a flame retardant (van der Veen and de Boer, 2012) and has been a known environmental contaminant for decades (Muir et al., 1980) occurring regularly in wastewater (Margot et al., 2015). It is often found in groundwater due to its extensive use in households though it degrades fairly rapidly and is not known to bioaccumulate (Funk et al., 2019).

Neotame was approved for use in the United States in 2002 (U.S. Food and Drug Administration, 2018) and has since been incorporated into a wide variety of food products and beverages (Aguilar et al., 2008). Because

it largely breaks down during metabolism (Margot et al., 2015), only trace amounts enter the environment. Therefore, it can serve as a powerful tracer of very recent or ongoing influx of wastewater effluent. Neotame was the most commonly detected CEC (n = 12) in this study which might be related to the extremely low detection limit for neotame (0.2 ng/L) versus other sweeteners (saccharin: 10 ng/L; acesulfame-K: 5 ng/L; aspartame: 1 ng/L). The occurrence of neotame in this study is in contrast to other studies that have not found neotame in wastewater effluent or groundwater though the detection limits in these other studies were orders of magnitude higher (Li et al., 2020; Margot et al., 2015). Notably, neotame was not found at any site in this study where denitrification was suspected, potentially because reducing conditions in the aquifer could result in the oxidation of neotame.

Neotame was related to $\delta^{15}N[NO_3]$ (r^2 = 0.64; Fig. S7) which indicates that it may be associated with wastewater. Neotame was also slightly correlated to HCO_3^- (r^2 = 0.55; Fig. S7) and Ca^{2+} (r^2 = 0.52; Fig. S7) at sites where it was detected. This is possibly the result of a septic or sewer source with high $\delta^{15}N[NO_3]$ values whereby denitrification causes an increase in HCO_3^- (Eq. (4)). Alternatively, nitrification of reduced N species associated with wastewater produces protons generating acidity (Eqs. (5) and (6)) causing the dissolution of carbonates (Menció et al., 2016). Both reactions are associated with a wastewater NO_3^- source.

$$2NH_3 + 3O_2 \rightarrow 2NO_2^- + 2H_2O + 2H^+ \quad (5)$$

$$NO_2^- + O_2 \rightarrow 2NO_3^- \quad (6)$$

Neotame was not correlated to Cl^-/Br^- or NO_3^-/Cl^- ratios. Unlike Cl^- and Br^-, neotame biodegrades in the environment, and its utility as a tracer is more related to its presence or absence rather than concentration. Where it was detected (Fig. S4), one can assume recent (post-2002) infiltration of an unknown proportion of wastewater.

5.4. Separating natural and anthropogenic recharge sources using ^3H, CEC, and ^{14}C

CECs were detected at six ^3H dead sites (Fig. 7; Table 1). ^3H does not re-equilibrate (and ^{14}C is very slow to re-equilibrate) with the atmosphere during recirculation of groundwater through infrastructure (Cook and Dogramaci, 2019). Groundwater recharged from leaky infrastructure will likely contain CECs, yet it may have different ^{14}C and ^3H values than naturally recharged groundwater. At two water-supply wells adjacent to KAFB, Travis et al. (2021) measured ^{14}C values of 37 and 27 PMC and no ^3H; they also found ^{14}C values decreased with depth and the deepest wells—screened ~80 m below the water table—had ^{14}C values between 7.6 and 12 PMC and no ^3H. Hence, groundwater recharged through leaky infrastructure in the field area on KAFB likely contains old ^{14}C, no ^3H, and CECs.

At groundwater sites that are ^3H dead with CEC detections and relatively low ^{14}C values (<55 PMC), recharge is likely occurring solely through leaky infrastructure and not modern recharge (Fig. 7A). In contrast, sites with measurable ^3H and higher PMC (Fig. 7B) may contain modern recharge from atmospheric precipitation or may be recharged from leaky infrastructure that contains ^3H and more modern ^{14}C. Using this qualitative assessment, only two sites (of 17 measured for ^3H, ^{14}C and CEC) show potential evidence of natural modern recharge (KAFB-0903 and Abandoned Chical). KAFB-0903 is in the northeast portion of Tijerras Arroyo (Fig. 1) and may receive infiltration through rainfall; the Abandoned Chical well is relatively shallow (~22 m surface to water level; southwest side of the study area on Isleta Pueblo) and contains geochemistry that suggests wastewater contamination (NO_3-N = 13.5, Cl/Br = 130, $\delta^{15}N[NO_3]$ = 10.1; Table 1). Sites likely recharged through leaky infrastructure (low ^{14}C values, ^3H dead, CEC detections), were generally on KAFB except for IP1 (located on the southern KAFB boundary near former sewage lagoons; Fig. 1). These artificial recharge sites generally had low NO_3^-/Cl^- (0.03 to 2.2; median 0.35) and variable Cl^-/Br^- ratios (63 to 172; median 77). Interestingly, KAFB-0514, which contains low concentrations of ^3H (2.13 pCi/L), a high NO_3^-/Cl ratio (2.2), and CECs may contain naturally occurring vadose zone NO_3^- mobilized during accidental sewer line releases (Section 5.1 and S.8.1). Hence at this site, a mix of recharge sources is likely.

Artificial recharge appears to affect all regions sampled. This includes sites where water levels were >150 m deep and had low ^{14}C values (<20 PMC). In this semi-arid environment, natural aquifer recharge likely only occurs at the mountain front boundary (Plummer et al., 2012) and through arroyos (Linhoff and Lunzer, 2021). Finding a near ubiquitous presence of CECs in groundwater beneath a thick vadose zone suggests leaky infrastructure is a major source of recharge to the aquifer.

6. Summary and conclusions

Determining the source of NO_3^- to groundwater is often difficult. This is especially true where there are multiple anthropogenic and natural NO_3^- sources known to contribute NO_3^- to groundwater. In this work, simple major ion ratios (Cl^-/Br^- and NO_3^-/Cl^-) proved a very useful first approximation for deciphering between anthropogenic and arid region vadose zone NO_3^- in groundwater. The highest NO_3^- concentrations corresponded to high NO_3^-/Cl^- (>1.5) and low Cl^-/Br^- ratios (<100), implying a subsoil NO_3^- source from the arroyo floodplains; this was further supported by NO_3^- isotope analysis ($\delta^{15}N[NO_3]$ < 8 ‰). In contrast, sites with elevated Cl^-/Br^- (>120) ratios generally had high $\delta^{15}N[NO_3]$ values (>8 ‰) and abundant CEC detections implying a wastewater NO_3^- source.

Natural attenuation of NO_3^- depends on the extent of denitrification happening in an aquifer (Nikolenko et al., 2018). In this study, where denitrification was occurring, reaction progress varied from 2 to 31 %

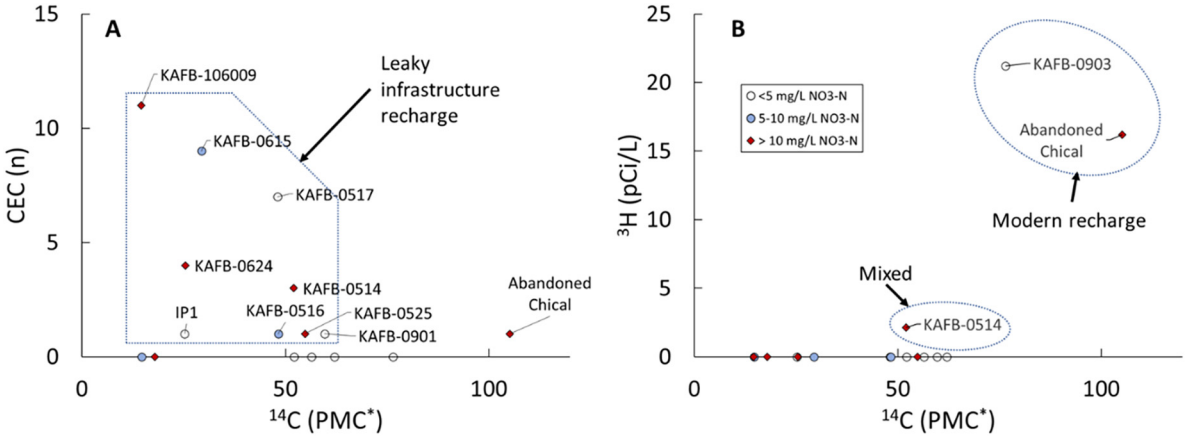

Fig. 7. The relationship between contaminants of emerging concern (CEC), ^{14}C, and ^3H. In this arid region, artificial recharge from leaky infrastructure is likely at sites with CEC detections, low ^{14}C, and no ^3H. Note, both panels show results from the same set of samples.

(Section 4.2 and Table S6). The dual isotope approach—analyzing both $\delta^{15}N[NO_3]$ and $\delta^{18}O[NO_3]$—showed that at least eight sites contained NO_3^- largely sourced from a wastewater or manure source (Fig. 2, Table 1). Most of these sites also contained reduced N species, elevated Cl^-/Br^- ratios, and CECs further suggesting a wastewater source. Where denitrification has occurred in the study area, $\delta^{13}C$ and major ion analyses suggest denitrification has oxidized organic carbon to produce HCO_3^-. With few exceptions, the general lack of denitrification across the field area demonstrates that NO_3^- likely behaves conservatively through most of the field area; hence, changes in ratios of NO_3^- to conservative ions such as Cl^- cannot be explained by denitrification and can be used to help differentiate NO_3^- sources. Further, due to the lack of denitrification, this work demonstrates that most of the elevated NO_3^- measured in the field area can be expected to persist. Readers interested in more detailed discussion of NO_3^- sources at individual sites are referred to S.8 and Table S3.

As the arroyo stream channel migrates across the floodplain over decades of monsoon seasons, subsoil NO_3^- reservoirs may periodically be flushed from subsoils and raise groundwater NO_3^- concentrations. It's also likely that in arroyo floodplains, irrigation, accidental sewer line releases, and leaky infrastructure will flush naturally occurring vadose zone NO_3^- to underlying aquifers exacerbating NO_3^- contamination. In many arid regions with thick unsaturated zones, groundwater recharge only naturally occurs through arroyos. The possibility that this recharge source could also periodically contain highly concentrated NO_3^- is concerning. While large subsoil NO_3^- reservoirs have not been observed outside of the floodplain of Tijeras Arroyo in this field area, similar reservoirs might also be present in many arroyo floodplains across the southwestern United States or in other arid settings. More research is needed to determine exactly where and how these NO_3^- reservoirs form and the extent of groundwater quality affected by this newly discovered NO_3^- source.

In this study, CECs were nearly ubiquitous across groundwater and surface waters and thus excellent indicators of recent recharge. Neotame emerged as a surprising tracer of very recent or ongoing infiltration of wastewater. It breaks down rapidly in the environment and was only approved for use in the United States in 2002 (U.S. Food and Drug Administration, 2018), hence it serves to help constrain the timing of recharge. However, because landfills, accidental sewer line releases, and septic systems all contribute CECs, it is difficult to decipher different anthropogenic NO_3^- sources based on CECs alone. Future studies could examine the CEC composition in transects moving downgradient of sewer line releases, septic leach fields, and landfills to determine whether the composition of CECs could be used in deciphering between types of anthropogenic wastewater sources. In this study, some sites with a very likely subsoil NO_3^- source (based on elemental ratios and $\delta^{15}N[NO_3]$) CECs were still detected. In these cases, either surface wastewater releases may have mobilized subsoil NO_3^- to the aquifer or the elevated NO_3^- concentrations are naturally occurring and CECs are infiltrating to the aquifer through runoff in the arroyo channel.

By combining CECs, ^3H, and ^{14}C, this study developed a potentially novel method of differentiating between natural and anthropogenic recharge. This method is only possible where supply wells pump pre-modern groundwater (^3H dead with low PMC), recharge does not naturally occur through the vadose zone following precipitation, and where CECs can be detected. In many arid settings—including most of the area in the present study—these qualifications are met. While the finding that leaky infrastructure plays a major role in recharge is not new (e.g., Lerner, 2002), this study shows it is substantial even beneath thick (>150 m) vadose zones in arid regions with limited natural recharge.

Supplementary data to this article can be found online at https://doi.org/10.1016/j.scitotenv.2022.157345.

Funding

This work was supported by the Air Force Civil Engineer Center.

CRediT authorship contribution statement

Benjamin Linhoff completed all conceptualization, data curation, formal analysis, funding acquisition, investigation, methodology design, and project administration. Furthermore, this manuscript was entirely written and edited by Benjamin Linhoff. Prior to submission, standard U.S. Geological Survey peer review was conducted by six internal U.S. Geological Survey scientists.

Declaration of competing interest

The authors declare that they have no known competing financial interests or personal relationships that could have appeared to influence the work reported in this paper.

Acknowledgements

Many people contributed to make this work possible. I would like to thank AECOM, Sandia National Laboratory, and Isleta Pueblo who supported sample collection. Helpful discussion of site selection and background work was provided by scientists from Sandia National Laboratory, the City of Albuquerque, Isleta Pueblo, New Mexico Environment Department, and Air Force Civil Engineer Center. Artificial sweetener method development was carried out by the Organic Geochemistry Research Laboratory at the U.S. Geological Survey Kansas Water Science Center. Lastly, I would like to thank the numerous reviewers of this work. Any use of trade, firm, or product names is for descriptive purposes only and does not imply endorsement by the U.S. Government.

References

Agency, U.S.E.P., 1981. Wastewater Treatment Facilities-Sludge Management System Albuquqerque, New Mexico.

Aguilar, F., Autrup, H., Barlow, S., Castle, L., Crebelli, R., Engel, K., Gontard, N., Gott, D., Grilli, S., Gürtler, R., Larsen, C., Leclercq, C., Leblanc, J., Malcata, F.X., Mennes, W., Milana, M.R., Pratt, I., Rietjens, I., Tobback, P., Toldrá, F., 2008. Neotame as a sweetener and flavour enhancer, scientific opinion of the panel on food additives , flavourings, processing aids and materials in contact with food. EFSA J. 1–43.

Bartolino, J.R., Anderholm, S.K., Myers, N.C., 2005. Groundwater resources of the East Mountain area, Bernalillo, Sandoval, Santa Fe, and Torrance Counties, New Mexico. U.S. Geological Survey Scientific Investigations Report 2009–5204 88.

Bexfield, L.M., Anderholm, S.K., 2002. Estimated Water-level Declines in the Santa Fe Group Aquifer System in the Albuquerque Area, Central New Mexico, Predevelopment to 2002. (p. 1)US Department of the Interior, US Geological Survey.

Bexfield, L.M., Toccalino, P.L., Belitz, K., Foreman, W.T., Furlong, E.T., 2019. Hormones and pharmaceuticals in groundwater used as a source of drinking water across the United States. Environ. Sci. Technol. 53, 2950–2960. https://doi.org/10.1021/acs.est.8b05592.

Böhlke, J.K., 2002. Groundwater recharge and agricultural contamination. Hydrogeol. J. 10, 153–179. https://doi.org/10.1007/s10040-001-0183-3.

Böhlke, J.K., Coplen, T.B., 1995. Interlaboratory Comparison of Secondary Reference Materials for Nitrogen-Isotope-Ratio Measurements, Technical Document. Int. Energy Vienna.

Böhlke, J.K., Ericksen, G.E., Revesz, K., 1997. Stable isotope evidence for an atmospheric origin of desert nitrate deposits in northern Chile and southern California, USA. Chem. Geol. 136 (1–2), 135–152. https://doi.org/10.1016/S0009-2541(96)00124-6.

Böhlke, J.K., Mroczkowski, S.J., Coplen, T.B., 2003. Oxygen isotopes in nitrate: new reference materials for $^{18}O:^{17}O:^{16}O$ measurements and observations on nitrate-water equilibration. Rapid Commun. Mass Spectrom. 17, 1835–1846. https://doi.org/10.1002/rcm.1123.

Böhlke, J.K., Wanty, R., Tuttle, M., Delin, G., Landon, M., 2002. Denitrification in the recharge area and discharge area of a transient agricultural nitrate plume in a glacial outwash sand aquifer, Minnesota. Water Resour. Res. 38, 10-1–10-26. https://doi.org/10.1029/2001wr000663.

Böttcher, J., Strebel, O., Voerkelius, S., Schmidt, H.-L., 1990. Using isotope fractionation of nitrate-nitrogen and nitrate-oxygen for evaluation of microbial denitrification in a sandy aquifer. J. Hydrol. 114, 413–424.

Buerge, I.J., Buser, H.-R., Kahle, M., Muller, M.D., Poiger, T., 2009. Ubiquitous occurrence of the artificial sweetener acesulfame in the aquatic environment: an ideal chemical marker of domestic wastewater in groundwater. Environ. Sci. Technol. 43, 4381–4385.

Canter, L.W., 1996. Nitrates in Groundwater. Routledge.

Cook, P.G., Dogramaci, S., 2019. Estimating recharge from recirculated groundwater with dissolved gases: an end-member mixing analysis. Water Resour. Res. 2019WR025012. https://doi.org/10.1029/2019WR025012.

Copland, J., 2019. Forensic Analyses and Nitrate Concentrations in Groundwater and the Suspected Nitrate Releases Sites in the Vicinity of SNL/NM and Northern KAFB, Albuquerque, New Mexico. Sandia National Laboratory Technical Memorandum and Plate, Albuquerque.

Copland, J.R., 2017. Well Construction Details, Groundwater Elevations, and Figures for the Tijeras Arroyo Groundwater Area at Sandia National Laboratories, New Mexico. https://doi.org/10.2172/1340634.
Coplen, T.B., 1994. Reporting of stable hydrogen, carbon, and oxygen isotopic abundances (technical report). Pure Appl. Chem. 66 (2), 273–276.
Davis, S.N., Whittemore, D.O., Fabryka-Martin, J., 1998. Uses of chloride/bromide ratios in studies of potable water. Ground Water https://doi.org/10.1111/j.1745-6584.1998.tb01099.x.
Eastoe, C.J., Watts, C.J., Ploughe, M., Wright, W.E., 2012. Future use of tritium in mapping pre-bomb groundwater volumes. Ground Water 50, 87–93. https://doi.org/10.1111/j.1745-6584.2011.00806.x.
Fishman, M.J., 1993. Methods of Analysis by the US Geological Survey National Water Quality Laboratory: Determination of Inorganic and Organic Constituents in Water and Fluvial Sediments (Vol. 93). US Department of the Interior, US Geological Survey.
Fahlberg, C., Remsen, I., 1879. On the oxidation of orthotoluene sulfamide. Rep. Ger. Chem. Soc. 12 (1), 469–473.
Food and Drug Administration, 2018. https://www.fda.gov/food/food-additives-petitions/additional-information-about-high-intensity-sweeteners-permitted-use-food-united-states. (Accessed 14 January 2022).
Funk, S.P., Duffin, L., He, Y., McMullen, C., Sun, C., Utting, N., Martin, J.W., Goss, G.G., Alessi, D.S., 2019. Assessment of impacts of diphenyl phosphate on groundwater and near-surface environments: sorption and toxicity. J. Contam. Hydrol. 221, 50–57.
Furlong, E.T., Noriega, M.C., Kanagy, L.K., Coffey, L.J., Burkhardt, M.R., 2014. Determination of human-use pharmaceuticals in filtered water by direct aqueous injection—high-performance liquid chromatography/tandem mass spectrometry, Chapter B10. U.S. Geological Survey Techniques and Methods, Book 5. U.S. Geological Survey https://doi.org/10.3133/tm5B10.
Galanter, A.E., Curry, L.T., 2019. Estimated 2016 Groundwater Level and Drawdown from Predevelopment to 2016 in the Santa Fe Group Aquifer System in the Albuquerque Area, Central New Mexico. U.S. Geological Survey Scientific Investigations Map 3433, 1 sheet, 13-p. pamphlet https://doi.org/10.3133/sim3433.
Gan, Z., Sun, H., Feng, B., Wang, R., Zhang, Y., 2013. Occurrence of seven artificial sweeteners in the aquatic environment and precipitation of Tianjin, China. Water Res. 47 (14), 4928–4937. https://doi.org/10.1016/j.watres.2013.05.038.
Geyh, M.A., 2000. An overview of 14C analysis in the study of groundwater. Radiocarbon 42, 99–114.
Glassmeyer, S.T., Koplin, D.W., Furlong, E.T., Focazio, M., 2008. Environmental Presence and Persistence of Pharmaceuticals: An Overview. Fate of Pharmaceuticals in the Environment and in Water Treatment Systems. U.S. Geological Survey, Boca Raton, pp. 3–51.
Gómez, R., Arce, M.I., Sánchez, J.J., del Mar Sánchez-Montoya, M., 2012. The effects of drying on sediment nitrogen content in a Mediterranean intermittent stream: a microcosms study. Hydrobiologia 679 (1), 43–59.
Graham, R.C., Hirmas, D.R., Wood, Y.A., Amrhein, C., 2008. Large near-surface nitrate pools in soils capped by desert pavement in the Mojave Desert, California. Geology 36, 259–262. https://doi.org/10.1130/G24343A.1.
Green, C.T., Puckett, L.J., Böhlke, J.K., Bekins, B.A., Phillips, S.P., Kauffman, L.J., Denver, J.M., Johnson, H.M., 2008. Limited occurrence of denitrification in four shallow aquifers in agricultural areas of the United States. J. Environ. Qual. 37, 994–1009. https://doi.org/10.2134/jeq2006.0419.
Grundl, T., Magnusson, N., Brennwald, M.S., Kipfer, R., 2013. Mechanisms of subglacial groundwater recharge as derived from noble gas, 14C, and stable isotopic data. Earth Planet. Sci. Lett. 369–370, 78–85. https://doi.org/10.1016/j.epsl.2013.03.012.
Gutiérrez, M., Biagioni, R.N., Alarcón-Herrera, M.T., Rivas-Lucero, B.A., 2018. An overview of nitrate sources and operating processes in arid and semiarid aquifer systems. Sci. Total Environ. 624, 1513–1522. https://doi.org/10.1016/j.scitotenv.2017.12.252.
Haase, C.S., Lozinsky, R.P., 1995. An underground view of the Albuquerque Basin. The Water Future of Albuquerque and Middle Rio Grande Basin: Proceedings of the 39th Annual New Mexico Water Conference: November 3–4, 1994, Albuquerque, New Mexico, p. 37.
Han, L.F., Plummer, L.N., 2016. A review of single-sample-based models and other approaches for radiocarbon dating of dissolved inorganic carbon in groundwater. Earth Sci. Rev. 152, 119–142. https://doi.org/10.1016/j.earscirev.2015.11.004.
Han, L.F., Plummer, L.N., Aggarwal, P., 2012. A graphical method to evaluate predominant geochemical processes occurring in groundwater systems for radiocarbon dating. Chem. Geol. 318–319, 88–112. https://doi.org/10.1016/j.chemgeo.2012.05.004.
Hollocher, T.C., 1984. Source of the oxygen atoms of nitrate in the oxidation of nitrite by Nitrobacter agilis and evidence against a P–O–N anhydride mechanism in oxidative phosphorylation. Arch. Biochem. Biophys. 233, 721–727.
Houlton, B.Z., Morford, S.L., Dahlgren, R.A., 2018. Convergent evidence for widespread rock nitrogen sources in Earth's surface environment. Science 360, 58–62. https://doi.org/10.1126/science.aan4399.
Izbicki, J.A., Flint, A.L., O'Leary, D.R., Nishikawa, T., Martin, P., Johnson, R.D., Clark, D.A., 2015. Storage and mobilization of natural and septic nitrate in thick unsaturated zones, California. J. Hydrol. 524, 147–165.
Jasechko, S., et al., 2017. Global aquifers dominated by fossil groundwaters but wells vulnerable to modern contamination. Nat. Geosci. 10, 425–430.
Katz, B.G., Eberts, S.M., Kauffman, L.J., 2011. Using Cl/Br ratios and other indicators to assess potential impacts on groundwater quality from septic systems: a review and examples from principal aquifers in the United States. J. Hydrol. 397, 151–166. https://doi.org/10.1016/j.jhydrol.2010.11.017.
Kendall, C., 1998. Chapter 16 - Tracing nitrogen sources and cycling in catchments. Isotope Tracers in Catchment Hydrology. Elsevier, pp. 519–576 https://doi.org/10.1016/B978-0-444-81546-0.50023-9.
Kendall, C., Aravena, R., 2000. Nitrate isotopes in groundwater systems. Environmental Tracers in Subsurface Hydrology. Springer, Boston, MA, pp. 261–297.
Kernodle, J.M., 1998. Simulation of ground-water flow in the Albuquerque Basin, central New Mexico, 1901-95, with projections to 2020. U.S. Geological Survey Open File Report 96-209 https://doi.org/10.3133/ofr96209.
Kroeger, K.D., Cole, M.L., Valiela, I., 2006. Groundwater-transported dissolved organic nitrogen exports from coastal watersheds. Limnol. Oceanogr. 51, 2248–2261. https://doi.org/10.4319/lo.2006.51.5.2248.
Lee, H.J., Kim, K.Y., Hamm, S.Y., Kim, M.S., Kim, H.K., Oh, J.E., 2019. Occurrence and distribution of pharmaceutical and personal care products, artificial sweeteners, and pesticides in groundwater from an agricultural area in Korea. Sci. Total Environ. 659, 168–176. https://doi.org/10.1016/j.scitotenv.2018.12.258.
Lerner, D.N., 2002. Identifying and quantifying urban recharge: a review. Hydrogeol. J. 10 (1), 143–152.
Li, D., Brien, J.W.O., Tscharke, B.J., Choi, P.M., Zheng, Q., Ahmed, F., Thompson, J., Li, J., Mueller, J.F., Sun, H., Thomas, K.V., 2020. National wastewater reconnaissance of artificial sweetener consumption and emission in Australia. Environ. Int. 143, 105963. https://doi.org/10.1016/j.envint.2020.105963.
Lindsey, B.D., Jurgens, B.C., Belitz, K., 2019. Tritium as an indicator of modern, mixed, and premodern groundwater age. U.S. Geological Survey Scientific Investigations Report 2019–5090 https://doi.org/10.3133/sir20195090 18 p.
Linhoff, B., Longmire, P., Rearick, M., McQuillan, D., Perkins, G., 2016. Water quality and hydrogeochemistry of a basin and range watershed in a semi-arid region of northern New Mexico. Environ. Earth Sci. 75, 640. https://doi.org/10.1007/s12665-015-5179-8.
Linhoff, B.S., Lunzer, J.J., 2021. Discovery of a large subsoil nitrate reservoir in an arroyo floodplain and associated aquifer contamination. Geology 1–5. https://doi.org/10.1130/G47916.1.
Lorite-Herrera, M., Hiscock, K., Jiménez-Espinosa, R., 2009. Distribution of dissolved inorganic and organic nitrogen in river water and groundwater in an agriculturally-dominated catchment, south-East Spain. Water Air Soil Pollut. 198, 335–346. https://doi.org/10.1007/s11270-008-9849-y.
Lowrance, R., 1992. Groundwater nitrate and denitrification in a coastal plain riparian forest. J. Environ. Qual. 21, 401–405. https://doi.org/10.2134/jeq1992.00472425002100030017x.
Luo, J., Zhang, Q., Cao, M., Wu, L., Cao, J., Fang, F., Li, C., Xue, Z., Feng, Q., 2019. Ecotoxicity and environmental fates of newly recognized contaminants-artificial sweeteners: a review. Sci. Total Environ. 653, 1149–1160. https://doi.org/10.1016/j.scitotenv.2018.10.445.
Margot, J., Rossi, L., Barry, D.A., Holliger, C., 2015. A review of the fate of micropollutants in wastewater treatment plants. WIREs Water 2, 457–487. https://doi.org/10.1002/wat2.1090.
Mariotti, A., 1983. Atmospheric nitrogen is a reliable standard for natural 15N abundance measurements. Nature 303, 685–687.
McCance, W., Jones, O.A.H., Cendón, D.I., Edwards, M., Surapaneni, A., Chadalavada, S., Wang, S., Currell, M., 2020. Combining environmental isotopes with Contaminants of Emerging Concern (CECs) to characterise wastewater derived impacts on groundwater quality. Water Res. 182, 116036. https://doi.org/10.1016/j.watres.2020.116036.
McCance, W., Jones, O.a.H, Edwards, M., Surapaneni, A., Chadalavada, S., Currell, M., 2018. Contaminants of emerging concern as novel groundwater tracers for delineating wastewater impacts in urban and peri-urban areas. Water Res. 146, 118–133. https://doi.org/10.1016/j.watres.2018.09.013.
McQuillan, D., 2004. Ground-water quality impacts from on-site septic systems. Proceedings, National Onsite Wastewater Recycling Association, 13th Annual Conference Albuquerque, pp. 1–13.
Menció, A., Mas-Pla, J., Otero, N., Regàs, O., Boy-Roura, M., Puig, R., Bach, J., Domènech, C., Zamorano, M., Brusi, D., Folch, A., 2016. Nitrate pollution of groundwater; all right…, but nothing else? Sci. Total Environ. https://doi.org/10.1016/j.scitotenv.2015.08.151.
Mohr, B.A., 2009. Feeling blue in the south valley: a case study of nitrate contamination in Albuquerque's south valley. Bull. Sci. Technol. Soc. 29, 408–420.
Muir, D.C.G., Grift, N.P., Blouw, A.P., Lockhart, W.L., 1980. Environmental dynamics of phosphate esters. I. Uptake and bioaccumulation of triphenyl phosphate by rainbow trout. Chemosphere 9, 525–532.
National Atmospheric Deposition Program (NRSP-3). 2022. NADP Program Office, Wisconsin State Laboratory of Hygiene, 465 Henry Mall, Madison, WI 53706, https://nadp.slh.wisc.edu/sites/ntn-nm07/, accessed on June 29, 2020.
Nikolenko, O., Jurado, A., Borges, A.V., Knöller, K., Brouyère, S., 2018. Isotopic composition of nitrogen species in groundwater under agricultural areas: a review. Sci. Total Environ. 621, 1415–1432. https://doi.org/10.1016/j.scitotenv.2017.10.086.
Nolan, B.T., Hitt, K.J., Ruddy, B.C., 2002. Probability of nitrate contamination of recently recharged groundwaters in the conterminous United States. Environ. Sci. Technol. 36, 2138–2145. https://doi.org/10.1021/es0113854.
Olsson, I.U., 1970. The use of oxalic acid as a standard. In: Olsson, I.U. (Ed.), Radiocarbon Variations and Absolute Chronology, Nobel Symposium, 12th Proc.John Wiley & Sons, New York, p. 17
Oneida Total Integrated Enterprises, 2014. Investigation Report SWMU ST-105 Nitrate Characterization.
Panno, S.V., Hackley, K.C., Hwang, H.H., Greenberg, S.E., Krapac, I.G., Landsberger, S., O'Kelly, D.J., 2006. Characterization and identification of Na-Cl sources in ground water. Ground Water 44, 176–187. https://doi.org/10.1111/j.1745-6584.2005.00127.x.
Patton and Kryskalla (2011).
Peng, X., Ou, W., Wang, C., Wang, Z., Huang, Q., Jin, J., Tan, J., 2014. Occurrence and ecological potential of pharmaceuticals and personal care products in groundwater and reservoirs in the vicinity of municipal landfills in China. Sci. Total Environ. 490, 889–898. https://doi.org/10.1016/j.scitotenv.2014.05.068.
Perakis, S.S., Hedin, L.O., 2002. Nitrogen loss from unpolluted South American forests mainly via dissolved organic compounds. Nature 415, 416–419.
Plummer, N., Bexfield, L.M., Anderholm, S.K., Sanford, W.E., Busenberg, Eurybiades, 2012. Geochemical characterization of ground-water flow in the Santa Fe group aquifer system, Middle Rio Grande Basin, New Mexico. USGS Water-Resour. Investig. Rep. 03-4131, pp. 1–395

Richardson, S.D., Ternes, T.A., 2011. Water analysis: emerging contaminants and current issues. Anal. Chem. 83 (12), 4614–4648. https://doi.org/10.1021/ac200915r.
Robertson, W.D., Cherry, J.A., 1992. Hydrogeology of an unconfined sand aquifer and its effect on the behavior of nitrogen from a large-flux septic system. Appl. Hydrogeol. 32–44.
Robertson, W.D., Van Stempvoort, D.R., Roy, J.W., Brown, S.J., Spoelstra, J., Schiff, S.L., Rudolph, D.R., Danielescu, S., Graham, G., 2016. Use of an artificial sweetener to identify sources of groundwater nitrate contamination. Groundwater 54, 579–587. https://doi.org/10.1111/gwat.12399.
Sapek, B., 2002. The impact of farmstead operation on groundwater quality. Int. Assoc. Hydrol. Sci. Publ. 125–130.
Scanlon, B., Reedy, R., Bronson, K., 2008a. Impacts of land use change on nitrogen cycling archived in semiarid unsaturated zone nitrate profiles, Southern High Plains, Texas. Environ. Sci. Technol. 42. https://doi.org/10.1021/es800792w.
Scanlon, B.R., Reedy, R.C., Bronson, K.F., 2008b. Impacts of land use change on nitrogen cycling archived in semiarid unsaturated zone nitrate profiles, southern High Plains, Texas. Environ. Sci. Technol. 42, 7566–7572. https://doi.org/10.1021/es800792w.
Schindler, D.W., 2006. Recent advances in the understanding and management of eutrophication. Limnol. Oceanogr. 51, 356–363. https://doi.org/10.4319/lo.2006.51.1_part_2.0356.
Schullehner, J., Hansen, B., Thygesen, M., Pedersen, C.B., Sigsgaard, T., 2018. Nitrate in drinking water and colorectal cancer risk: a nationwide population-based cohort study. Int. J. Cancer 143 (1), 73–79. https://doi.org/10.1002/ijc.31306.
Sherris, A.R., Baiocchi, M., Fendorf, S., Luby, S.P., Yang, W., Shaw, G.M., 2021. Nitrate in drinking water during pregnancy and spontaneous preterm birth: A retrospective within-mother analysis in California. Environ. Health Perspect. 129 (5). https://doi.org/10.1289/EHP8205.
Sigman, D.M., Casciotti, K.L., Andreani, M., Barford, C., Galanter, M., Böhlke, J.K., 2001. A bacterial method for the nitrogen isotopic analysis of nitrate in seawater and freshwater. Anal. Chem. 73, 4145–4153. https://doi.org/10.1021/ac010088e.
Spalding, R.F., Exner, M.E., 1993. Occurrence of nitrate in groundwater—a review. J. Environ. Qual. 22, 392–402. https://doi.org/10.2134/jeq1993.00472425002200030002x.
Stites, W., Kraft, G.J., 2001. Nitrate and chloride loading to groundwater from an irrigated North-Central U.S. Sand-Plain Vegetable Field. J. Environ. Qual. 30, 1176–1184. https://doi.org/10.2134/jeq2001.3041176x.
Taylor, M., Clarke, W.P., Greenfield, P.F., 2003. The treatment of domestic wastewater using small-scale vermicompost filter beds. Ecol. Eng. 21, 197–203. https://doi.org/10.1016/j.ecoleng.2003.12.003.
Thomson, B.M., McQuillan, D.M., 1984. Nitrate contamination of groundwater in Albuquerque. Sel. Pap. Water Qual. Pollut. N. M.
Tran, N.H., Li, J., Hu, J., Ong, S.L., 2014. Occurrence and suitability of pharmaceuticals and personal care products as molecular markers for raw wastewater contamination in surface water and groundwater. Environ. Sci. Pollut. Res. 21, 4727–4740.
Travis, R.E., Bell, M.T., Linhoff, B.S., Beisner, K.R., 2021. Utilizing multiple hydrogeologic and anthropogenic indicators to understand zones of groundwater contribution to water-supply wells near Kirtland Air Force Base Bulk Fuels Facility in southeast Albuquerque, New Mexico. U.S. Geological Survey Scientific Investigations Report 2021–5076 28 https://doi.org/10.3133/sir20215076.
U.S. Environmental Protection Agency (EPA), 2021. National primary drinking water regulations. Washington DC [accessed 2021 July] Available from https://www.epa.gov/ground-water-and-drinking-water/national-primary-drinking-water-regulations#Organic.
U.S. Geological Survey, 2022. USGS water data for the Nation: U.S. Geological Survey National Water Information System database. accessed [January 10, 2022], at https://doi.org/10.5066/F7P55KJN.
van der Veen, I., de Boer, J., 2012. Phosphorus flame retardants: properties, production, environmental occurrence, toxicity and analysis. Chemosphere 88, 1119–1153.
Van Stempvoort, D.R., Brown, S.J., Bickerton, G., 2011. Artificial sweeteners as potential tracers in groundwater in urban environments. J. Hydrol. 401 (1–2), 126–133. https://doi.org/10.1016/j.jhydrol.2011.02.013.
Vidal-Dorsch, D.E., Bay, S.M., Maruya, K., Snyder, S.A., Trenholm, R.A., Vanderford, B.J., 2012. Contaminants of emerging concern in municipal wastewater effluents and marine receiving water. Environ. Toxicol. Chem. 31 (12), 2674–2682. https://doi.org/10.1002/etc.2004.
Walvoord, M.A., 2010. A reservoir of nitrate beneath. Science 1021, 1021–1025. https://doi.org/10.1126/science.1086435.
Walvoord, M.A., Phillips, F.M., Stonestrom, D.A., Evans, R.D., Hartsough, P.C., Newman, B.D., Striegl, R.G., 2003. A reservoir of nitrate beneath desert soils. Science 302. https://doi.org/10.1126/science.1086435.
Ward, M.H., Jones, R.R., Brender, J.D., De Kok, T.M., Weyer, P.J., Nolan, B.T., Villanueva, C.M., Van Breda, S.G., 2018. Drinking water nitrate and human health: an updated review. Int. J. Environ. Res. Public Health 15 (7). https://doi.org/10.3390/ijerph15071557.
Weiss, R.F., 1970. The solubility of nitrogen, oxygen and argon in water and seawater. Deep-Sea Res. Oceanogr. Abstr. 721–735.
Zaugg, S.D., Smith, S.G., Schroeder, M.P., 2006. Determination of wastewater compounds in whole water by continuous liquid–liquid extraction and capillary-column gas chromatography/mass spectrometry, Chapter B4. U.S. Geological Survey Techniques and Methods, Book 5. U.S. Geological Survey https://doi.org/10.3133/tm5B4.
Zhang, Q., Sun, J., Liu, J., Huang, G., Lu, C., Zhang, Y., 2015. Driving mechanism and sources of groundwater nitrate contamination in the rapidly urbanized region of south China. J. Contam. Hydrol. 182, 221–230.